This article has been accepted for publication in a future issue of this journal, but has not been fully edited. Content may change prior to final publication. Citation information: DOI 10.1109/OJCOMS.2020.3015394, IEEE Open Journal of the Communications Society



# Channel Estimation Techniques for Millimeter-Wave Communication Systems: Achievements and Challenges

Kais Hassan, Mohammad Masarra, Marie Zwingelstein and Iyad Dayoub, Senior Member IEEE

***Abstract*—The fifth-generation (5G) of cellular networks and beyond requires massive connectivity, high data rates, and low latency. Millimeter-wave (mmWave) communications is a key 5G enabling technology to meet these requirements thanks to its technical potentials that can be integrated with other 5G enablers such as ultra-dense networks (UDNs) and massive multiple-input-multiple-output (massive MIMO) systems. However, some technical challenges, which are mainly related to specific characteristics of mmWave propagation, must be addressed. All the aforementioned points will be discussed in this paper before presenting the different existing architectures of massive MIMO mmWave systems. This survey mainly aims at presenting a comprehensive state-of-the-art review of the channel estimation techniques associated with the different mmWave system architectures. Subsequently, we will provide a comparison among existing solutions in terms of their respective benefits and shortcomings. Finally, some open directions of research are discussed, and challenges that wait to be met are pointed out.**

***Index Terms*—Millimeter-wave communications, massive MIMO, channel estimation, 5G, cellular systems, spatial channel model, lens antenna array, hybrid architecture, few-bit ADCs, compressive sensing, beamforming.**

## NOMENCLATURE

| | |
|---|---|
| **2D** | Two Dimensional |
| **3D** | Three Dimensional |
| **4G** | Fourth Generation |
| **5G** | Fifth Generation |
| **AAVE** | Antenna Array with Virtual Elements |
| **ADC** | Analog-to-Digital Converter |
| **AMP** | Approximate Message Passing |
| **AoA** | Angle-of-Arrival |
| **AoD** | Angle-of-Departure |
| **AWGN** | Additive White Gaussian Noise |
| **BiG-AMP** | Bilinear Generalized Approximate Message Passing |
| **BIHT** | Binary Iterative Hard Thresholding |
| **BS** | Base Station |
| **CMOS** | Complementary Metal Oxide Semiconductor |
| **C-OMP** | Covariance Orthogonal Matching Pursuit |
| **CoSaMP** | Compressive Sampling Match Pusuit |
| **CP** | CANDECOMP/PARAFAC |
| **CS** | Compressive Sensing |
| **CSI** | Channel State Information |
| **DC** | Dual Crossing |
| **DC-OMP** | Dynamic Covariance Orthogonal Matching Pursuit |
| **DCS** | Distributed Compressed Sensing |
| **DFT** | Discrete Fourier Transform |
| **DGMP** | Distributed Grid Matching Pursuit |
| **DL** | DownLink |
| **DS-OMP** | Dynamic Simultaneous Orthogonal Matching Pursuit |
| **EM** | Expectation-Maximization |
| **FBMC** | Filter Bank based Multi-Carrier |
| **FDD** | Frequency-Division Duplexing |
| **FFT** | Fast Fourier Transform |
| **GAMP** | Generalized Approximate Message Passing |
| **GOMP** | Generalized Orthogonal Matching Pursuit |
| **IHT** | Iterative Hard Thresholding |
| **JCE+LS** | Joint Channel Estimation + Local Search |
| **LASSO** | Least Absolute Shrinkage and Selection Operator |
| **LMMSE** | Linear Minimum Mean Squared Estimator |
| **LOS** | Line-of-Sight |
| **LSE** | Least-Squares Estimation |
| **MG-OMP** | Multi-Grid Orthogonal Matching Pursuit |
| **MIMO** | Multiple-Input Multiple-Output |
| **MMP** | Multipath Matching Pursuit |
| **MMSE** | Minimum Mean Square Error |
| **mmWave** | Millimeter-Wave |
| **M-OMP** | Multiple Measurement Vector Orthogonal Matching Pursuit |
| **MRC** | Maximum Ratio Combining |
| **MT** | Mobile Terminal |
| **MU** | Multi-User |
| **MUSIC** | MUltiple SIgnal Classification |
| **NLOS** | Non-Line-of-Sight |
| **OFDM** | Orthogonal Frequency-Division Multiplexing |
| **OMP** | Orthogonal Matching Pursuit |
| **RF** | Radio-Frequency |
| **RX** | Receiver |
| **SC-FDE** | Single Carrier-Frequency Domain |

K. Hassan is with Le Mans University, 72085 Le Mans, France, Laboratoire d'Acoustique de l'Universit du Mans (LAUM) - UMR CNRS 6613, 72085 Le Mans, France (e-mail: kais.hassan@univ-lemans.fr).

M. Masarra, M. Zwingelstein and I. Dayoub are with University Polytechnic Hauts-de-France, CNRS, Univ. Lille, ISEN, Centrale Lille, UMR 8520 - IEMN - Institut D'Electronique de Microlectronique Et de Nanotechnologie - DOAE - Dpartement Opto-Acousto-Electronique, F59313 Valenciennes, France (e-mail: Mohammad.Masarra@uphf.fr, marie.zwingelstein-colin@uphf.fr, iyad.dayoub@uphf.fr).

This work is licensed under a Creative Commons Attribution 4.0 License. For more information, see https://creativecommons.org/licenses/by/4.0/.

This article has been accepted for publication in a future issue of this journal, but has not been fully edited. Content may change prior to final publication. Citation information: DOI 10.1109/OJCOMS.2020.3015394, IEEE Open Journal of the Communications Society



| | |
|---|---|
| | Equalization |
| **SdMP** | Stage-Determined Matching Pursuit |
| **SINR** | Signal-to-Interference-plus-Noise Ratio |
| **SISO** | Single-Input Single-Output |
| **SNR** | Signal-to-Noise Ratio |
| **S-OMP** | Simultaneous Orthogonal Matching Pursuit |
| **SSAMP** | Structured Sparsity Adaptive Matching Pursuit |
| **SS-SW-OMP+Th** | Subcarrier Selection SW-OMP + Thresholding |
| **SU** | Single-User |
| **SURE** | Stein's Unbiased Risk Estimate |
| **SVD** | Singular Value Decomposition |
| **SW-OMP** | Simultaneous Weighted Orthogonal Matching Pursuit |
| **TDD** | Time-Division Duplexing |
| **TX** | Transmitter |
| **UL** | UpLink |
| **ULA** | Uniform Linear Array |
| **ULPA** | Uniform Linear Planar Array |
| **VAMP** | Vector Approximate Message Passing |
| **ZF** | Zero Forcing |

## I. Introduction and Background

The next decade will encounter many emerging applications such as connected cars, augmented reality, virtual reality, mixed reality, 3D video, ultra-high definition video, industrial IoT, smart cities, connected healthcare, etc. These applications require to massively connect new devices and to exchange more data. For instance, the global mobile traffic is expected to grow annually by 30 percent between 2018 and 2024, and the capacity demand in the next decade is expected to witness a 1000-fold increase [1]. Among the fifth generation (5G) promises, when compared to fourth generation (4G), is to increase user data rate by 10 to 100 (up to 10 Gbit/s), to reduce latency by 10, to increase connectivity density by 10, and also to reduce the cost and power consumption [2]. Due to this hugely increasing demand for data traffic and massive connectivity as well as to the scarcity in the sub-6 GHz radio spectrum, researchers are trying to propose new solutions. These are mainly based either on the new signal processing techniques, or on densifying the network, or on exploiting additional frequency bands.

In regards of exploiting new bands, the millimeter-wave (mmWave) spectrum is between 30 GHz and 300 GHz (i.e. wavelengths between 1mm to 10mm) where the large unused bandwidth in these bands can allow the wireless systems to support the enormously increase in capacity demand since capacity of wireless systems increases when the exploited bandwidth increases. Hence, mmWave communications will play an essential role in 5G and upcoming future generations of cellular networks [3]–[6].

Despite their bandwidth attractivity, mmWave communications systems suffer from high free-space path-loss when compared to the sub-6 GHz ones. In addition, a substantial attenuation is observed in some mmWave bands due to atmospheric absorption, and rain and snow effects. Therefore, the mmWave signal risks to propagate over a few meters in some scenarios, and hence mmWave communications may be only suitable for very close-range communications such as in indoor applications. This difficulty can be overcome for outdoor mobile communications, where a greater transmission range is expected, by either increasing the transmission power or by using high-gain, high-directional antennas. Since the transmission power is always limited by regulations, mmWave systems must enable narrow steering beams such as the transmitter and the receiver steer towards each other which results in high directional gain in the wanted directions and low gain in the unwanted ones. The desirable high directivity is based on signal processing techniques such as beamforming which requires to increase the number of antennas of the antenna arrays at the transmitter and/or receiver, i.e. massive antenna arrays are needed. This approach is facilitated by the short wavelength of mmWave signals which makes possible to compact more antennas while keeping the array size small. Another aspect of mmWave system design comes from the impossibility to directly apply the traditional digital transceiver architectures, which are employed in sub-6 GHz, directly to mmWave systems because of the high power consumption of mmWave radio-frequency (RF) chains. Recently, new tailored multiple-input-multiple-output (MIMO) architectures were proposed to solve this problem namely *fully-analog*, *hybrid* and *few-bit ADCs* architectures. The objective is to reduce the total consumed power by either reducing the number of RF chains or the power consumption per each one.

Hence, mmWave communications are a key technology enabler for the soon expected 5G and beyond, not only thanks to the huge available bandwidth, but also by means of its complementary with other 5G enablers such as ultra-dense networks (UDNs) and massive MIMO. MmWave links are suitable for wireless backhauling and short-range communications in the small cells of UDNs while still capable of mitigating interferences by using the high-directional antenna arrays. This high directivity is enabled by the beamforming ability of massive MIMO. However, the evolution of mmWave communications is hindered by challenges that require more insight to propose the needed solutions to reach their full potential. Some of these challenges come from the propagation characteristics in the mmWave bands (the path-loss, penetration loss, and the atmospheric attenuation), others come from the high power consumption and the hardware impairments of mmWave circuits.

### *The contributions of the survey*

An important part of any telecommunications system is *channel estimation* which is essential to optimize link performance. Acquiring channel state information (CSI) is particularly challenging for mmWave systems because of the massive number of antennas, the complex architecture of the transceiver and the large exploited bandwidth.

The aim of this survey is to propose a comprehensive overview of the existing channel estimation techniques for

This work is licensed under a Creative Commons Attribution 4.0 License. For more information, see https://creativecommons.org/licenses/by/4.0/.

This article has been accepted for publication in a future issue of this journal, but has not been fully edited. Content may change prior to final publication. Citation information: DOI 10.1109/OJCOMS.2020.3015394, IEEE Open Journal of the Communications Society



Table I
REVIEW OF THE MAIN TOPICS STUDIED IN THE EXISTING SURVEYS ON MMWAVE COMMUNICATIONS SYSTEMS

| | |
|---|---|
| Access and Coverage | [5] |
| Channel Estimation | [5], [8], [12] |
| Channel Measurement | [5], [6], [12] |
| Channel Modelling | [5]–[7], [12] |
| Cross-Layer Design | [10], [12] |
| Key Challenges and Technical Potentials | [3], [5] |
| MIMO Architecture | [4], [5], [9] |
| Performance Analysis | [4] |
| Propagation Characteristics | [3], [4], [6], [7] |
| Standardization | [10], [12] |

mmWave systems. We attempt to present each estimation method in a clear and concise manner while providing sufficient level of details to offer a fair comparison among them in terms of performance, studied scenario, and MIMO architecture design. The studied scenario concerns the different assumptions that were considered in existing research works, such as i) is it a single-user or a multi-user system? ii) is the channel a frequency-selective channel? iii) which duplexing mode is used? iv) is it a 2D or 3D channel estimation? v) which channel model is adopted? etc. One important thing to note is that the channel estimation techniques are generally tailored to the MIMO architecture of the transmitter and receiver, as well as to the employed antenna array. As a result, some methods are powerful when used with planar array antenna and hybrid architecture but their performance will degrade when it comes to lens antenna array systems or to few-bit analog-to-digital converters (ADCs) ones.

To the best of our knowledge, there has been no survey that discussed the channel estimation methods for mmWave systems, although there are few surveys available such as [3]–[15] which typically overview mmWave systems without specifically dealing with the channel estimation aspect. Table I shows a review of some topics related to mmWave systems and the surveys in which each topic was largely reviewed. For instance, a chapter in [8] was dedicated to present six channel estimation papers which were published between 2014 and 2016. Some channel estimation papers with hybrid architecture were reviewed in [5], [12]. However, a further inclusive review of this aspect is needed. In particular, channel estimation techniques with few-bit ADCs architecture, and with lens antenna were not considered in the above mentioned surveys.

### *Scope and Organization*

This inclusive survey focuses on the channel estimation methods for mmWave communication systems and provides a summary of the latest research progress in this domain. The outline of this paper can be summarised as:

- First, in section II the characteristics of mmWave channels such as the differences between the propagation behavior in the mmWave bands and in the sub-6 GHz ones are illustrated. This will help to understand the technical potential of mmWave communications, the challenges which have to be addressed to reach this potential, and the enabler-technologies to reply to these challenges.
- Then in section III, we discuss the different existing system architectures which are proposed for massive MIMO mmWave systems. The spatial MIMO channel models which present the special nature of highly-directive mmWave communications are also introduced before presenting the massive MIMO system model.
- Afterwards, compressive sensing (CS) as a mathematical tool for channel estimation is presented in section IV.
- In the following sections, the channel estimation techniques for mmWave systems are comprehensively reviewed. It is organised as follows: Existing channel estimation techniques for hybrid architecture, for lens antenna array architecture, and for few-bit ADCs architectures are respectively introduced in section V, section VI and section VII. Conclusions are offered at the end of each section.
- The learned lessons are presented in section VIII before identifying some open research directions. Finally, section IX completes the paper with concluding remarks.

The skeleton structure of our survey is illustrated in figure 1.

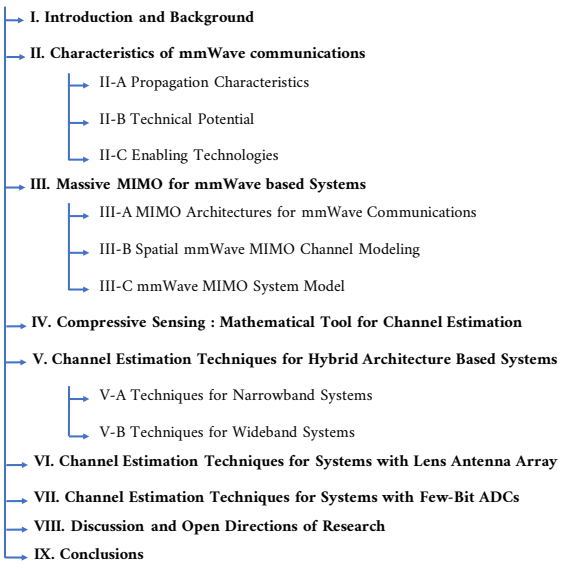


Figure 1. The outline of this survey.

### *Notation*

Lightface letters denote scalars. Boldface lower- and uppercase letters denote column vectors and matrices, respectively. $[\mathbf{A}]_{n,m}$ and $\mathbf{x}_i$ stand for the entries of matrix $\mathbf{A}$ and vector $\mathbf{x}$, respectively. $[\mathbf{A}]_{n,:}$ is the $n^{\text{th}}$ row of matrix $\mathbf{A}$. The $M \times M$ identity matrix is $\mathbf{I}_M$. $\mathbf{1}_M$ is an $M \times 1$ unity vector. The Kronecker product of matrix $\mathbf{A}$ and matrix $\mathbf{B}$ is expressed as $\mathbf{A} \otimes \mathbf{B}$ . $\mathbf{A}^H$ is the Hermitian (conjugate transpose) of matrix $\mathbf{A}$. $\|\mathbf{x}\|_0$ is the number of non-zero entries of the vector $\mathbf{x}$. $E[\cdot]$ is the statistical expectation. Letter $j$ is the imaginary unit, i.e., $j^2 = -1$. $\lceil x \rceil$ denotes the ceiling function. An ellipsis "..." refers to the continuation of an equation. Finally, $a \propto b$ means $a$ is proportional to $b$.

This work is licensed under a Creative Commons Attribution 4.0 License. For more information, see https://creativecommons.org/licenses/by/4.0/.

This article has been accepted for publication in a future issue of this journal, but has not been fully edited. Content may change prior to final publication. Citation information: DOI 10.1109/OJCOMS.2020.3015394, IEEE Open Journal of the Communications Society



## II. Characteristics of mmWave communications

An increased attention has recently been drawn to the huge spectrum in the mmWave frequency bands to meet the increase in the global mobile data traffic and to achieve up of hundreds of times more capacity compared to current 4G cellular networks [16]–[18].

MmWave communications have been employed for applications such as radar and point-to-point communication for 100 years ago [19] . In the last decade, some mmWave standards have emerged including IEEE 802.15.3c [20], IEEE 802.11ad [21] and WirelessHD [22] which are intended to wireless personal area networks, wireless local area networks and wireless HDMI, respectively. Recently, the mobile network research community dedicated a lot of atention to the sub-100 GHz systems operating in the 28 GHz, 38 GHz, 60 GHz, 71 GHz and 81 GHz bands, while the band above 100 GHz has been studied by only a few very recent papers [23]. Some proof of concept studies had been conducted in the last years. In May 2013, Samsung realized a 1.056 Gb/s transmission in the 28 GHz band to a distance of up to 2 km [24]. In April 2015, a peak rate of 15 Gbps at 73 GHz was achieved by Nokia in collaboration with National Instruments [5]. In February 2018, Deutsche Telekom and Huawei have successfully completed the world's first multi-cell field tests at 73 GHz [25].

However, the propagation characteristics at mmWave frequencies are different from that at the traditional sub-6 GHz ones, that is why we will show in the following subsections the main technical advantages and challenges of the mmWave technology.

### A. Propagation Characteristics

A major difference between sub-6 GHz and mmWave systems in terms of propagation characteristics is in their free-space path-loss ($\mathrm{PL_{FS}}$) [26] which is described by,

$$\mathrm{PL_{FS}} \propto \frac{d^n}{\lambda^2}, \tag{1}$$

where $d$ is the distance between the transmitter and receiver, $n$ is the path-loss exponent which typically equals 2, and $\lambda$ is the wavelength of the signal. However, $n$ is less than 2 in some scenarios of cellular networks and indoor applications [27]. On the other hand, path-loss exponent can reach the value of 6 in some severe environments of propagation [28]. A comparison between the microwave propagation in the 1.8 GHz GSM band and the mmWave one in the 73 GHz bands, under the same configuration (transmission distance, propagation environment, antenna array), shows an additional loss of 32 dB in the mmWave band [29]. Recent urban model experiments also show a degradation of 40 dB in path-loss at 28 GHz compared to 2.8 GHz [28], [30]. Thus, the severe path-loss of mmWave propagation required to be compensated by a strong directionality.

The *atmospheric* attenuation of mmWave signals, which is caused particularly by the absorption of oxygen and water vapor, as well as the scattering of rain, must be added to the path-loss. The atmospheric attenuation depends on the operating frequency. The atmospheric oxygen absorption is especially severe at 60 GHz and 120 GHz, and the water vapor absorption is particularly very high at 180 GHz [31]. Also, rain attenuation at mmWave frequencies is much greater than that of sub-6 GHz frequencies [32].

Another factor which affects the propagation of mmWave signals is their severe penetration loss which results in susceptibility to the static and dynamic blockage effect. In fact, some obstacles, such as human bodies, doors, glass and walls, attenuate and even can block mmWaves signals. For instance, attenuation of a 28 GHz signal can be as high as 24 dB and 45 dB if penetrating respectively through two walls and four doors [33]. Hence, it is not realistic to employ outdoor base stations (BSs) to serve indoor users for example.

The severe path-loss, the vulnerability of mmWave transmissions to blockages, and the atmospheric attenuation affect the choice of the operating frequencies, and require important changes to the system design and architecture.

### B. Technical Potential

Despite the challenging characteristics of the mmWave channel, mmWave communications will be an important part of the 5G cellular system and beyond. This is due to the potential of mmWave communications in terms of large bandwidth availability and short wavelength.

*Large bandwidth:* The 5G requirements for very high data rate communications may not be achievable by focusing only on the heavily-occupied conventional sub-6 GHz frequency bands. On the contrary, an abandon of the mmWave bands is available to be exploited opening the door to multi-Gigabit data exchange in spite of the low spectral efficiency since a very large bandwidth is hopefully sufficient to support very high data rates [34]. For instance, more than 12 GHz of bandwidth is available between 60 GHz and 90 GHz which is also called the E-band. Furthermore, the low spectral efficiency means less complexity and more robustness making mmWave systems more feasible. Actually, the 3rd Generation Partnership Project (3GPP) Release 15 selected the 24∼29 GHz and 37∼43 GHz frequency bands for the deployment of 5G mmWave systems [35]. In the future, the International Telecommunication Union (ITU) and the 3GPP will allocate two frequency bands around 40 GHz and 100 GHz for commercial use [13]. In July 2016, the Federal Communications Commission (FCC) dedicated several mmWave bands for wireless services including around 28 GHz and 39 GHz for licensed allocation, and 64∼71 GHz for unlicensed usage [36].

*Short wavelength:* The short wavelength is the main reason behind the strong path-loss of mmWave signals and hence the need for high directivity antennas which can be realised with antenna arrays and beamforming techniques. Narrower beams require higher number of antennas in the array which is compatible with mmWave communications thanks to the short wavelength. Indeed, the shorter the wavelength is, the smaller the antenna arrays' sizes are (since the distance between any two antennas in the array is basically half of the wavelength) and thus the higher the number of antennas to be packed into the same physical array size is, and also the higher the beamforming gain is [5], [13], [16]. It is worth noting that a typical

This work is licensed under a Creative Commons Attribution 4.0 License. For more information, see https://creativecommons.org/licenses/by/4.0/.

This article has been accepted for publication in a future issue of this journal, but has not been fully edited. Content may change prior to final publication. Citation information: DOI 10.1109/OJCOMS.2020.3015394, IEEE Open Journal of the Communications Society



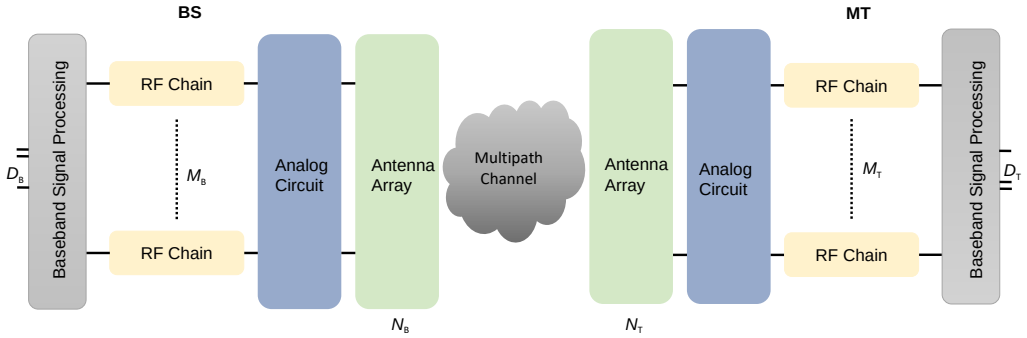


Figure 2. General system architecture of mmWave transceiver.

antenna length at 60 GHz is less than 2.5 mm for example [13]. Another benefit of highly directional communications, based on narrow beams at the transmitter and at receiver, is that it helps to secure the mmWave communication link against eavesdropping and jamming as well as to increase the interference immunity [5], [37].

### C. Enabling Technologies

The mmWave communications technology is, at the same time, enabled by and complementary to some other technologies such as massive MIMO, advances in signal processing, network densification and finally advances in circuit design and integration.

*Massive MIMO:* The use of a large number of antennas at BSs and for mobile terminals (MTs) is called Massive MIMO and is an essential technology to increase the capacity of cellular networks. Massive MIMO has been studied for conventional sub-6 GHz systems, and is also very crucial for mmWave systems where high directivity is mandatory [38]. Higher frequency bands offered by mmWave systems grant the ability to design antenna arrays with a huge number of antennas [39]. However, this will not be possible without the recent advances in complementary metal oxide semiconductor (CMOS) circuits which increase the capacity of circuit integration [40].

*Enhanced Signal Processing Techniques:* It is clear that the conventional *fully-digital* MIMO system, in which one RF chain is dedicated to each antenna, is infeasible for mmWave systems because of the high implementation cost and high energy consumption [18], [41], [42]. Indeed, it has been shown that RF components can consume up to 70% of the total transceiver power consumption [43]. For these reasons, several mmWave *hybrid* architectures were proposed as alternatives to the fully-digital one, see section III-A. These solutions offer a good balance between system performance and hardware complexity. However, they require to develop new signal processing techniques for beamforming, channel estimation, and more generally for improving system performance.

*Network Densification:* Network densification means increasing the density of BSs deployment in the network via several tiers and an hierarchy of macro, micro, pico and femto cells, and leads to a multi-tier heterogeneous network [44]. Increasing the small cells density increases capacity and spectral efficiency of served users at the expense of increasing the cost of interference management [45]. MmWave communications are a very good candidate for small cell deployment mainly for three reasons i) a small cell means a short-range communication which makes the high path-loss of mmWave communications less unfavorable, ii) the larger bandwidth of mmWave frequencies means higher capacity which is the main goal of small cells deployment, iii) and the high directivity of mmWave communications, at the transmitter and receiver, results in better interference control.

## III. Massive MIMO for mmWave Systems

Millimeter-wave communication systems need to employ a large number of antennas at the transmitter and receiver sides. Some early research works suggested arrays of 32 to 256 antennas at the BS and 4 to 16 ones at the mobile terminal [17], [46]. Fortunately, it is now possible to pack such number of antennas into small packages [47], [48]. However, other aspects such as the power consumption and cost influence the maximum number of antennas that can be integrated in the mmWave system. If digital signal processing techniques are employed for baseband precoding at the transmitter (TX) and combining at the receiver (RX) then one dedicated RF chain per antenna is needed, where each RF chain includes an ADC. These techniques are usually used for sub-6 GHz systems. However, they are not affordable actually at mmWave frequencies as the bandwidths become wider and the antenna arrays become larger. This results in high-resolution ADCs and high energy consumption of each RF chain. For instance, 30 mW per RF chain is consumed at sub-6 GHz frequencies, while 250 mW per RF chain is needed at mmWave frequency bands [18].

Figure 2 is a block diagram that illustrates the general architecture of a hybrid mmWave transceiver. Without loss of generality, a BS equipped with $M_{\mathrm{B}}$ RF chains and $N_{\mathrm{B}}$ antennas ($M_{\mathrm{B}} < N_{\mathrm{B}}$) is assumed to communicate with an MT equipped with $M_{\mathrm{T}}$ RF chains and $N_{\mathrm{T}}$ antennas ($M_{\mathrm{T}} < N_{\mathrm{T}}$) in order to exchange some data streams [4]. In practice, the number of RF chains at the MTs is usually less than that at the BSs. A point to point communication is considered here, however, this architecture could be easily extended to the case of multi-users. The combined role of the baseband digital processing and the analog circuit of the hybrid architecture

This work is licensed under a Creative Commons Attribution 4.0 License. For more information, see https://creativecommons.org/licenses/by/4.0/.

This article has been accepted for publication in a future issue of this journal, but has not been fully edited. Content may change prior to final publication. Citation information: DOI 10.1109/OJCOMS.2020.3015394, IEEE Open Journal of the Communications Society



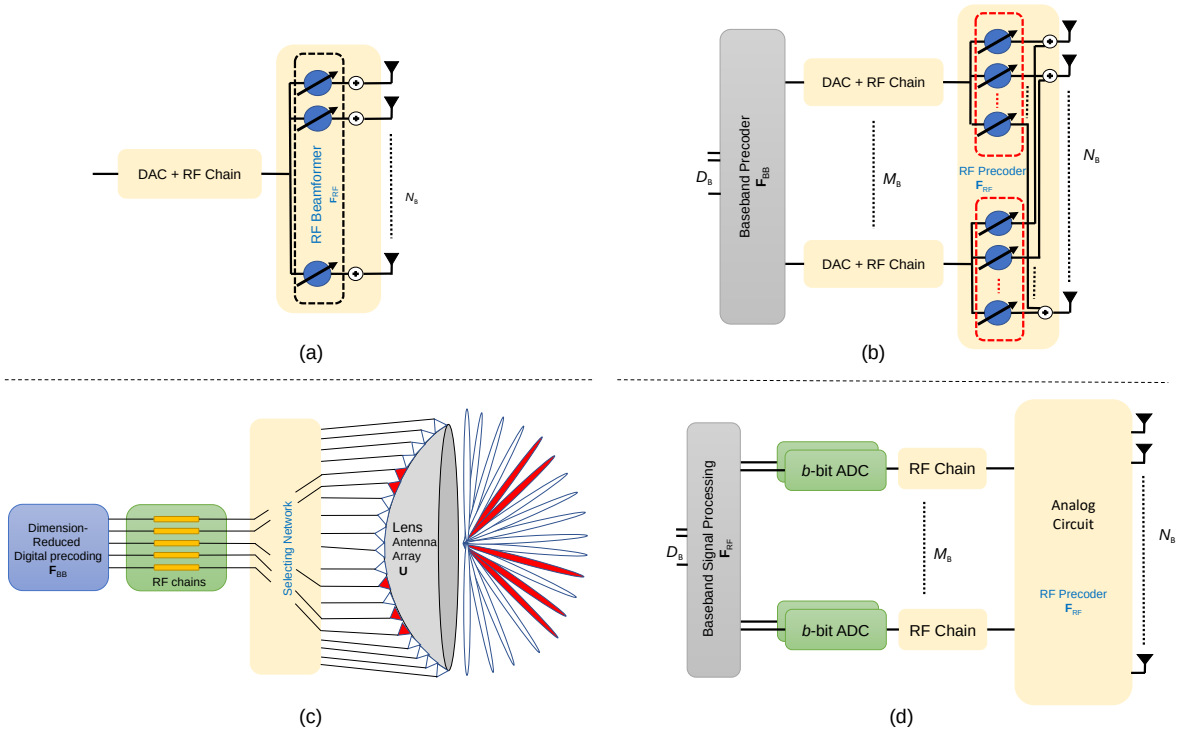


Figure 3. Different MIMO architectures (a) fully-analog architecture; (b) hybrid architecture; (c) lens array architecture (d) few-bit ADCs architecture .

is to direct the beams at the transmitter or/and receiver. In contrast with the traditional fully-digital architecture that does not consider an analog circuit behind (before) the RF chains at the transmitter (receiver) and considers one RF chain per antenna, i.e. $M_{\mathrm{B}} = N_{\mathrm{B}}, M_{\mathrm{T}} = N_{\mathrm{T}}$ [5], [49]. For this reason, fully-digital architecture must be avoided nowadays when it comes to mmWave communication systems although it could be possible at some point in the future. This leads to introducing some new hybrid architectures in order to make the massive MIMO mmWave systems feasible. The idea is to figure out how to reduce the number of RF chains and the resolution of the ADCs which consequently will reduce the total power consumption and the total cost. Different transceiver architectures for mmWave communication will be introduced in the following section.

### A. MIMO Architectures for mmWave Communications

*Fully-Analog Architecture:* One solution is to reduce the number of RF chains to one and to perform beamforming entirely using the analog processing. As illustrated in figure 3(a) [5], [49], this is achieved by analog shifters employed in the RF domain to adjust the phase of the RF signals at each antenna. This solution drastically reduces the hardware cost and power consumption.

Many studies have been carried out on the *fully-analog* architecture. A codebook-based analog beamformer for mmWave wireless personal area networks via beam switching is discussed in [50]. [51], [52] which propose an alternative codebook-based beamforming for outdoor backhaul based on a joint transmitter-receiver beam scanning employing a tree-structured codebook. Moreover, an iterative channel estimation and analog beamforming algorithm has been investigated in [53]–[56], where the coefficients at the transmitter and receiver sides are calculated to reach asymptotically singular value decomposition (SVD) elements.

Unfortunately, these solutions suffer from hardware limitations due to the constant modulus constraint imposed by the implementation of the phase shifters, hence the signals can only be partially adjusted [5], [49]. Another drawback of the fully-analog architecture is that it supports only one data stream, which makes its usage for multi-user communications tricky. However, this architecture is still a good fit for some standards such as WirelessHD for instance.

*Hybrid Architecture:* The hybrid architecture represents a compromise between the fully-digital architecture (where the number of RF chains equals that of the antennas) and the fully-analog one (where only one RF chain is employed). Precoding (at the transmitter) and combining (at the receiver) are performed in both the analog and the digital domains as shown in figure 3(b). The idea is to employ a dimension-reduced precoder/combiner with a small number of RF chains ($M_{\mathrm{B}} \ll N_{\mathrm{B}}, M_{\mathrm{T}} \ll N_{\mathrm{T}}$) while still relying on full-size analog precoder/combiner. Despite the reduced number of RF chains, the performance of these architectures has been shown to be not far from the fully-digitally ones [18], [46], [57]. This can be explained by the sparse nature of the mmWave channel (since the number of scatters is small), which makes the channel matrix low-rank [6], [58], see section IV for further illustration about sparsity. In addition, this solution supports easily several users/data streams, their number being equal or less than the number of RF chains. The 3GPP included the hybrid architecture in its recommendation for 5G systems in

This work is licensed under a Creative Commons Attribution 4.0 License. For more information, see https://creativecommons.org/licenses/by/4.0/.

This article has been accepted for publication in a future issue of this journal, but has not been fully edited. Content may change prior to final publication. Citation information: DOI 10.1109/OJCOMS.2020.3015394, IEEE Open Journal of the Communications Society



2016 [59].

Furthermore, the analog processing (precoding/combining) can be realized through different analog networks with phase shifters, namely the fully-connected networks [60] and the sub-connected ones [46], [61]. The idea is either to connect each RF chain to all the antennas, or to connect it to a subset of them. It seems that the sub-connected choice could be practically more interesting since it reduces the cost and complexity while still achieving a good performance when compared to the fully-connected network [46], [61], [62]. Another alternative is to replace the phase shifters (and all the required complementary components such as power combiners/splitters, control lines) with switches [62], [63]. Using switching networks could reduce the power consumption and complexity at the expense of lesser spectral-efficiency. One perspective is to combine switches and phase shifters to obtain an advantageous trade-off between them [64].

*Lens Array Architecture:* All the above mentioned architectures consider 1D or 2D planar antenna arrays. An attractive emerging approach is to combine *lens antenna arrays* with switching networks [65], [66]. A lens array is an electromagnetic lens with feed antennas located on the focal surface of the lens, which allows to concentrate the signal arriving from different directions on different antennas as depicted in figure 3(c). Hence, the spatial model of the channel can be seen as a beamspace model. Furthermore, the beamspace of mmWave channels is sparse since the scattering is not rich and the power is propagated over a small number of paths [6], [58]. Due to the sparsity of the mmWave channel, a reduced-size switching network is used to select the dominant beams in the beamspace, which greatly reduces the number of RF chains [65], [66]. The authors in [66] had shown that the number of required switches (or RF chains) to achieve near-optimal capacity in lens array systems depends on the number of signal beams (and not on the number of antennas on the lens), and they proposed a spatial multiplexing scheme for mmWave communications, namely the path-division multiplexing.

*Few-Bit ADCs Architecture:* Reducing the power consumption can be done either by reducing the number of RF chains (as proposed in the above presented architectures) and/or by reducing the energy consumed per RF chain. The latest is the key motivation behind proposing to replace the high-resolution ADCs with few-bit (e.g., 1 to 4 bit) ADCs, since high-frequency high-resolution ADCs are well known to consume a lot of power [18], [67], [68]. The mmWave system with few-bit ADCs is shown in figure 3(d). Using few-bit ADCs could even open the door to the feasibility of fully-digital mmWave systems [18]. However, the high non-linearity errors of quantization and the wide bands of mmWave channels pose a lot of challenges to the design of signal processing solutions for mmWave communications despite some recent research works [69], [70].

### B. Spatial mmWave MIMO Channel Modeling

MmWave channel models are classified into two categories [6], physical models and analytical models. The physical models are based on the electromagnetic characteristics of the signal propagation between the transmit and receive antenna arrays. They can efficiently reflect the measured parameters and they are popular for MIMO channels, hence they are a good choice for mmWave MIMO channels. On the other hand, the analytical models are based on the mathematical analysis of the channel, and they are convenient for algorithm development and system analysis. The physical channel models are divided into two categories. Deterministic models, which characterize the real effects of the environment on the system, but need high computational complexity, and stochastic channel models, which require low computational complexity, hence they are the popular choice for mmWave system design and simulation. Thus the considered channel model for this paper is the Saleh-Valenzuela stochastic channel model.

Since the number of scatters is limited [6], [58], most research works had adopted the geometric channel model to describe mmWave channels [4], [60], [61]. Let us consider again the system presented in figure 2. In the geometric channel model, the $N_{\mathrm{T}} \times N_{\mathrm{B}}$ complex matrix $\mathbf{H}_{\mathrm{DL}}$ of the narrowband downlink (DL) channel is expressed as,

$$\mathbf{H}_{\mathrm{DL}} = \sqrt{\frac{N_{\mathrm{B}} N_{\mathrm{T}}}{L \alpha_{\mathrm{PL,DL}}}} \sum_{l=1}^{L} \alpha_{l,\mathrm{DL}} \mathbf{a}_{\mathrm{T}} \left(\theta_{l,\mathrm{T}}, \phi_{l,\mathrm{T}}\right) \mathbf{a}_{\mathrm{B}}^{H} \left(\theta_{l,\mathrm{B}}, \phi_{l,\mathrm{B}}\right), \tag{2}$$

where $L$ is number of paths between the BS and MT ($L$ is small), $\alpha_{\mathrm{PL,DL}}$ is the average path-loss, $\alpha_{l,\mathrm{DL}}$ is the complex gain of the $l^{th}$ path in the DL channel, and $(\theta_{l,\mathrm{T}}, \phi_{l,\mathrm{T}})$ and $(\theta_{l,\mathrm{B}}, \phi_{l,\mathrm{B}})$ are the azimuth and elevation angles of arrival (AoAs) and the azimuth and elevation angles of departure (AoDs) respectively. Finally, $\mathbf{a}_{\mathrm{B}}$ ($\mathbf{a}_{\mathrm{T}}$) is the $N_{\mathrm{B}} \times 1$ ($N_{\mathrm{T}} \times 1$) complex antenna array response (steering) vector at the BS (at the MT). Spatially quantized AoDs and AoAs can be employed to represent the channel over the whole space, i.e. $\theta_{l,\mathrm{T}}, \phi_{l,\mathrm{T}}, \theta_{l,\mathrm{B}}, \phi_{l,\mathrm{B}}$ can be obtained from a uniform grid of $N_{\mathrm{G}}$ points on $[0, 2\pi[$ with $N_{\mathrm{G}} \gg L$ [71], [72]. This approach is also called the virtual MIMO channel representation [73]. In this approach, the channel in (2) can be reformulated as,

$$\mathbf{H}_{\mathrm{DL}} = \mathbf{A}_{\mathrm{T}} \mathbf{H}_{\alpha} \mathbf{A}_{\mathrm{B}}^{H}, \tag{3}$$

where $\mathbf{A}_{\mathrm{B}} \in \mathbb{C}^{N_{\mathrm{B}} \times L}$ and $\mathbf{A}_{\mathrm{T}} \in \mathbb{C}^{N_{\mathrm{T}} \times L}$ are, respectively, the aggregation of the $L$ steering vectors $\mathbf{a}_{\mathrm{B}}\left(\theta_{l,\mathrm{T}}, \phi_{l,\mathrm{T}}\right)$ and $\mathbf{a}_{\mathrm{T}}\left(\theta_{l,\mathrm{T}}, \phi_{l,\mathrm{T}}\right)$ for $l = 1, 2, \cdots, L$, and $\mathbf{H}_{\alpha} = \sqrt{\frac{N_{\mathrm{B}} N_{\mathrm{T}}}{L \alpha_{\mathrm{PL}}}} \mathrm{diag}\left(\alpha_{1,\mathrm{DL}}, \alpha_{2,\mathrm{DL}}, \cdots, \alpha_{L,\mathrm{DL}}\right)$.

The channel is frequency-selective when the system is wideband, hence equation (2) must be rewritten to represent the $D$-delay DL channel model. The $d$-th delay tap is given by [74],

$$\mathbf{H}_{\mathrm{DL}}(d) = \sqrt{\frac{N_{\mathrm{B}} N_{\mathrm{T}}}{L \alpha_{\mathrm{PL,DL}}}} \sum_{l=1}^{L} \alpha_{l,\mathrm{DL}} p_{\mathrm{B}}\left(dT_s - \tau_l\right) \ldots \mathbf{a}_{\mathrm{T}}\left(\theta_{l,\mathrm{T}}, \phi_{l,\mathrm{T}}\right) \mathbf{a}_{\mathrm{B}}^{H}\left(\theta_{l,\mathrm{B}}, \phi_{l,\mathrm{B}}\right), \tag{4}$$

where $p_{\mathrm{B}}(.)$ is the combination of pulse shaping filter and other filters at the BS, $T_s, \tau_l$ are the sampling period and the delay. For orthogonal frequency-division multiplexing (OFDM) mod-

This work is licensed under a Creative Commons Attribution 4.0 License. For more information, see https://creativecommons.org/licenses/by/4.0/.

This article has been accepted for publication in a future issue of this journal, but has not been fully edited. Content may change prior to final publication. Citation information: DOI 10.1109/OJCOMS.2020.3015394, IEEE Open Journal of the Communications Society



ulation, the MIMO channel frequency response matrix at each subcarrier $k$ follows the expression [74],

$$\mathbf{H}_{\mathrm{DL}}(k) = \sqrt{\frac{N_{\mathrm{B}} N_{\mathrm{T}}}{L \alpha_{\mathrm{PL,DL}}}} \sum_{l=1}^{L} \alpha_{l,\mathrm{DL}} q_l(k) \ldots \mathbf{a}_{\mathrm{T}}(\theta_{l,\mathrm{T}}, \phi_{l,\mathrm{T}}) \mathbf{a}_{\mathrm{B}}^{H}(\theta_{l,\mathrm{B}}, \phi_{l,\mathrm{B}}), \quad (5)$$

where $q_l(k)$ is given by,

$$q_l(k) = \sum_{d=1}^{D} p_{\mathrm{B}}(dT_s - \tau_l) e^{-\frac{2\pi j k d}{K_s}}, \quad (6)$$

and $K_s$ is the number of subcarriers.

The response vectors for two antenna array configurations, namely the uniform linear planar array (ULPA) and the lens array, are given as follows.

*ULPA Response Vector:* A ULPA is a rectangular array that consists of $N_h$ antennas in each row and $N_v$ antennas in each column, in the horizontal and vertical directions, uniformly separated by a distance $d$. Typically, $d = \lambda/2$ where $\lambda$ is the signal wavelength. The total number of antennas within the array is $N = N_h \times N_v$, and each row or column is a uniform linear array (ULA) which is considered as a special case of ULPA. The response vector of an $N$-element ULA is given by,

$$\mathbf{a}_{\mathrm{ULA}}(\theta) = \frac{1}{\sqrt{N}} \left[1 \; e^{j2\pi \frac{d}{\lambda} \sin(\theta)} \; \cdots \; e^{j(N-1)2\pi \frac{d}{\lambda} \sin(\theta)}\right]^{T} \quad (7)$$

The array response for the ULPA configuration is given by [75], [76],

$$\mathbf{a}_{\mathrm{ULPA}}(\theta, \phi) = \mathbf{a}_h(\theta) \otimes \mathbf{a}_v(\phi) \quad (8)$$

where $\theta$ and $\phi$ are, respectively, the azimuth and elevation angles, and $\mathbf{a}_h$ and $\mathbf{a}_v$ are the horizontal and vertical steering vectors which are derived from (7) with the corresponding angle and number of antennas.

Recently, 3D beamforming techniques for mmWave communications had been introduced [77]–[79]. However, few papers studied the estimation of the 3D mmWave channel [80]–[82]. On the other hand, most existing research works had considered only the 2D beamforming case, i.e. the elevation is neglected and only the horizontal scattering is taken into consideration. Under these assumptions, the ULPA response is rewritten as,

$$\mathbf{a}_{\mathrm{ULPA}}(\theta) = \mathbf{a}_h(\theta) \otimes \mathbf{1}_{N_v} \quad (9)$$

where $\mathbf{1}_{N_v}$ is an $N_v \times 1$ unity vector.

*Lens Array Response Vector:* Modeling the lens antenna array is typically based on separating the energy-focusing electromagnetic lens from the feeding antenna array where the lens effect is approximated by a spatial discrete Fourier transform (DFT) matrix, $\mathbf{U}$, of size $N \times N$ [65], [81]–[84]. The DFT matrix is composed of $N$ orthogonal array response vectors steering towards $N$ beams scanning the entire space, and is defined as [65], [82],

$$[\mathbf{U}]_{i \times j,:} = [\mathbf{a}(\xi_i, \xi_j)]^{H}, \quad (10)$$

where $\xi_i = \frac{1}{N_h}\left(i - \frac{N_h+1}{2}\right)$ for $i = 1, 2, \cdots, N_h$, $\xi_j = \frac{1}{N_v}\left(j - \frac{N_v+1}{2}\right)$ for $j = 1, 2, \cdots, N_v$, and $N_h$,$N_v$ are, respectively, the number of horizontal and vertical antennas of the lens array ($N = N_h \times N_v$). The idea is that this special antenna configuration transforms the above presented spatial channel into a beamspace model. This allows us to apply a beam selection technique in the beamspace domain directly without affecting the width of beams nor the gain of the antenna pattern. This model is referred to as the *DFT model*.

Another approach for modeling lens antenna arrays is to study the lens and the matching antenna array as one integrated unit and to derive an approximated closed-form of the array response vector [66], [85], [86]. The 3D lens antenna array can steer towards given azimuth and elevation angles, $\theta$ and $\phi$, based on the following response vector [85],

$$a_m(\theta, \phi) = e^{-j\phi_0} \sqrt{\tilde{D}_h \tilde{D}_v} \mathrm{sinc}\left(m_v - \tilde{D}_v \sin\phi\right) \ldots \mathrm{sinc}\left(m_h - \tilde{D}_h \sin\theta \cos\phi\right), \quad (11)$$

where $m_h = 1, \pm 1, \pm 2, \cdots \pm \frac{N_h - 1}{2}$ and $m_v = 1, \pm 1, \pm 2, \cdots \pm \frac{N_v - 1}{2}$ are the horizontal and vertical indices of each antenna . $\tilde{D}_h \triangleq \frac{D_h}{\lambda}$ and $\tilde{D}_v \triangleq \frac{D_h}{\lambda}$ denote the electric dimensions of the lens which are the physical dimensions, $D_h$ and $D_v$, normalized by the wavelength, and $\phi_0$ is a common phase shift from the lens aperture to the array. This model is referred to as the *approximated array response model*.

### C. mmWave MIMO System Model

Let us first consider a narrowband system model for a hybrid architecture. The downlink is described by the $N_{\mathrm{T}} \times 1$ received signal vector at the MT, which is given by

$$\mathbf{r}_{\mathrm{T}} = \mathbf{H}_{\mathrm{DL}} \mathbf{F}_{\mathrm{B}} \mathbf{S}_{\mathrm{B}} + \mathbf{n}, \quad (12)$$

where $\mathbf{H}_{\mathrm{DL}}$ is the DL channel matrix as defined in equation (2), $\mathbf{S}_{\mathrm{B}}$ is the $D_{\mathrm{B}} \times 1$ normalized transmitted symbols vector with $E\left[\mathbf{S}_{\mathrm{B}} \mathbf{S}_{\mathrm{B}}^{H}\right] = (P_{\mathrm{B}}/D_{\mathrm{B}}) \mathbf{I}_{D_{\mathrm{B}}}$, and $P_{\mathrm{B}}$ is the average transmission power of the BS. Also, $\mathbf{F}_{\mathrm{B}} = \mathbf{F}_{\mathrm{RF,B}} \mathbf{F}_{\mathrm{BB,B}}$ is the $N_{\mathrm{B}} \times D_{\mathrm{B}}$ precoding matrix of the BS which combines the baseband precoder $\mathbf{F}_{\mathrm{BB,B}} \in \mathbb{C}^{M_{\mathrm{B}} \times D_{\mathrm{B}}}$ and the RF precoder $\mathbf{F}_{\mathrm{RF,B}} \in \mathbb{C}^{N_{\mathrm{B}} \times M_{\mathrm{B}}}$. Finally, the vector $\mathbf{n}$ of size $N_{\mathrm{T}} \times 1$ is the additive white Gaussian noise (AWGN). The received vector $\mathbf{r}$ is processed at the MT such as,

$$\mathbf{y}_{\mathrm{T}} = \mathbf{W}_{\mathrm{T}}^{H} \mathbf{H}_{\mathrm{DL}} \mathbf{F}_{\mathrm{B}} \mathbf{S}_{\mathrm{B}} + \mathbf{W}_{\mathrm{T}}^{H} \mathbf{n}, \quad (13)$$

where $\mathbf{W}_{\mathrm{T}} = \mathbf{W}_{\mathrm{RF,T}} \mathbf{W}_{\mathrm{BB,T}}$ is the $N_{\mathrm{T}} \times D_{\mathrm{T}}$ combiner matrix of the MT which is assumed to consecutively apply the RF combiner $\mathbf{W}_{\mathrm{RF,T}} \in \mathbb{C}^{N_{\mathrm{T}} \times M_{\mathrm{T}}}$ and the baseband combiner $\mathbf{W}_{\mathrm{BB,T}} \in \mathbb{C}^{M_{\mathrm{T}} \times D_{\mathrm{T}}}$ . It is worth noting that the constant modulus constraint must be applied to the RF precoder and to the RF combiner when analog shifters are used, that is all the entries of the matrix must have the same magnitude. Finally, the channel matrix $\mathbf{H}_{\mathrm{DL}}$ in (13) must be replaced by the beamspace channel matrix, $\tilde{\mathbf{H}}_{\mathrm{DL}}$, in the case of lens antenna array, when the lens effect is separately modeled as in equation (10), where $\tilde{\mathbf{H}}_{\mathrm{DL}} = \mathbf{U}\mathbf{H}_{\mathrm{DL}}$.

This work is licensed under a Creative Commons Attribution 4.0 License. For more information, see https://creativecommons.org/licenses/by/4.0/.

This article has been accepted for publication in a future issue of this journal, but has not been fully edited. Content may change prior to final publication. Citation information: DOI 10.1109/OJCOMS.2020.3015394, IEEE Open Journal of the Communications Society



The same logic can be employed for the uplink (UL) by replacing $\mathbf{H}_{\mathrm{DL}}$ by the UL channel matrix $\mathbf{H}_{\mathrm{UL}}$ and by reversing the combiners and precoders roles. Under the widely-adopted assumption of *channel reciprocity* [87], the UL channel is a Hermitian transposition of the DL channel $\mathbf{H}_{\mathrm{UL}} = \mathbf{H}_{\mathrm{DL}}^{H}$, and one between them must be estimated to have CSI [8]. In practice, it is not obvious how to guarantee the channel reciprocity in mmWave communications, even for time-division duplexing (TDD) systems (where the same carrier frequency is used for both DL and UL), due to different issues, for instance the synchronization and calibration errors of RF chains [8]. However, it should be pointed out that the number of paths and the AoAs/AoDs for each path are strongly correlated for both DL and UL channels even for frequency-division duplexing (FDD) communication systems where separated DL and UL frequencies are employed. This property is called the *path reciprocity* [86]. Assuming path reciprocity, the $N_{\mathrm{B}} \times N_{\mathrm{T}}$ complex matrix $\mathbf{H}_{\mathrm{UL}}$ of the UL channel is given by,

$$\mathbf{H}_{\mathrm{UL}} = \sqrt{\frac{N_{\mathrm{B}} N_{\mathrm{T}}}{L \alpha_{\mathrm{PL,UL}}}} \sum_{l=1}^{L} \alpha_{l,\mathrm{UL}} \mathbf{a}_{\mathrm{T}} \left(\theta_{l,\mathrm{T}}, \phi_{l,\mathrm{T}}\right) \mathbf{a}_{\mathrm{B}}^{H} \left(\theta_{l,\mathrm{B}}, \phi_{l,\mathrm{B}}\right), \tag{14}$$

where $\alpha_{l,\mathrm{UL}}$ is the complex gain of the $l^{th}$ path in the UL channel, and is in general different from $\alpha_{l,\mathrm{DL}}$ as introduced in Equation (2).

For wideband systems, equation (13) is reformulated to express the received signal at each subcarrier $k$. It is rewritten as

$$\mathbf{y}_{\mathrm{T}}(k) = \mathbf{W}_{\mathrm{T}}^{H}(k) \mathbf{H}_{\mathrm{DL}}(k) \mathbf{F}_{\mathrm{B}}(k) \mathbf{S}_{\mathrm{B}}(k) + \mathbf{W}_{\mathrm{T}}^{H}(k) \mathbf{n}(k), \tag{15}$$

where $\mathbf{H}_{\mathrm{DL}}(k)$ is given by (5).

In the following sections, we will explain why the CS techniques are good candidates to estimate the sparse mmWave channels. Afterword, an inclusive review of existing channel estimation methods for mmWave systems with hybrid architecture, with lens antenna array, and with few-bit ADCs, is respectively presented in section V, section VI and section VII.

## IV. Compressive Sensing : Mathematical Tool for Channel Estimation

The multi-path signal components of mmWave systems tend to be distributed into few clusters such as mmWave channels look sparse [60], [75], [88]. This sparsity characteristic is also verified by measurements, for instance, [28], [30], [89], [90] showed that mmWave channels typically exhibit only 3-4 scattering clusters in dense-urban non-line-of-sight (NLOS) environments. Thus a convenient representation of such channels needs a comprehensive study of sparsity. The traditional training-based channel estimation methods seem to be not optimal under these sparse conditions due to the huge channel size (big number of antennas at the TX and RX) and the fact that most of what we get will be thrown away. Hence, the aim is to estimate the non-zero elements of the channel and one approach to solve this type of problems is to use CS techniques [91]–[93]. CS is widely employed in wireless communication applications like channel estimation, spectrum sensing for cognitive radio, and localization among others [94]. CS tools handle the problem of estimating any sparse signal by directly acquiring a compressive signal representation with a lot fewer number of samples than that required by the Shannon-Nyquist theorem, and from which the sparse signal can be recovered through an optimization process [92], [95].

A signal represented by an $n \times 1$ vector $\mathbf{s} \in \mathbb{C}^n$ is said to be exactly $k$-sparse signal if all but just $k \ll n$ values in the vector are zeros, in other words, there is a very small number of non-zero values in the vector and the rest are zero value elements. Mathematically, we can represent it as $\|\mathbf{s}\|_0 \leq k$. The same idea can be generalized to 2D and 3D signals. Consider a discrete-time signal $\mathbf{x}$, which can be represented by an $n \times 1$ vector in $\mathbb{C}^n$. If $\mathbf{x}$ is not sparse, it can be transformed into another domain via a transformation matrix $\mathbf{\Psi} \in \mathbb{C}^{n \times n}$ as follows

$$\mathbf{x} = \mathbf{\Psi s} \tag{16}$$

such as $\mathbf{s}$ represents an exactly $k$-sparse signal. It is very essential to employ a careful transformation matrix which can further expose the sparse nature of the original signal.

The objective of CS tools is to compress the dimension of measurements by projecting the high-dimensional sparse signals of dimension $n$ into a reduced-dimension spaces of dimension $m \ll n$ via a measurement or sensing matrix $\mathbf{\Phi}$ such as

$$\mathbf{y} = \mathbf{\Phi x} = \mathbf{\Phi \Psi s} = \mathbf{\Theta s} \tag{17}$$

where $\mathbf{\Theta} = \mathbf{\Phi \Psi}$ is an $m \times n$ matrix. This requires first to design a stable sensing (measurement) matrix $\mathbf{\Phi}$, and consequently a matrix $\mathbf{\Theta}$, before proposing a reconstruction algorithm to recover the signal $\mathbf{x}$ from only $m \approx k$ measurement vector $\mathbf{y}$ with the best reconstruction reliability and hence the minimum information loss. This problem is ill-posed in general, but can be resolved for the class of signals that have a sparse expansion. This requires that the design of the compression matrix $\mathbf{\Theta}$ respects some properties such as *the restricted isometry property* and *the small coherence* [96]–[98]. The first represents a necessary and sufficient condition for the CS problem to be well conditioned, while the later makes the CS technique more effective.

Many algorithms have been proposed to recover $k$-sparse signals with high probability [99], where some of them used tractable mixed-norm optimization methods [100]–[102], efficient greedy algorithms [98], [103]–[105], fast iterative thresholding methods [106], statistical sparse recovery [107], and many more [94], [95], [108], [109]. We give a glance and point out some of these algorithms. The non-convex $\ell_0$-norm problem is transformed into a convex $\ell_1$-norm one, and basis pursuit (BP) solutions [100], such as least absolute shrinkage and selection operator (LASSO) [102], are used. However, the BP approach is rarely implemented in real-time wireless applications because of its high computational cost. Orthogonal matching pursuit (OMP) is a greedy algorithm [98] which was proposed as an effective alternative to the BP ones [100]. In [105], compressive sampling matching pursuit (CoSaMP), which is a parallel greedy algorithm, was introduced. Moreover, the authors in [104] proposed a modified version of the OMP, called multi-grid OMP (MG-OMP), in

This work is licensed under a Creative Commons Attribution 4.0 License. For more information, see https://creativecommons.org/licenses/by/4.0/.

This article has been accepted for publication in a future issue of this journal, but has not been fully edited. Content may change prior to final publication. Citation information: DOI 10.1109/OJCOMS.2020.3015394, IEEE Open Journal of the Communications Society



order to reduce the complexity, and to make the reconstruction more adaptive. Another low-complexity approach, which tries to solve the problem by iteratively refining the sparse estimate, is a thresholding approach illustrated in [106]. Three algorithms were proposed in [110]–[112] that select more than one candidate per iteration to decrease the running time, while for OMP one candidate is selected per each iteration. An algorithm termed as multipath matching pursuit (MMP) was proposed in [110], where it performs the tree search, in which all combinations of $k$-sparse indices are the candidates in the tree, and the algorithm tries to find the best candidate from this tree that minimizes the residual. The aforementioned algorithm imposes reasonable computational overhead while achieving better performance over existing greedy algorithms. A generalization algorithm of the OMP was proposed in [111] termed as generalized OMP (GOMP) that selects more than one index per iteration corresponding to largest correlation in magnidute with the residual. Similar to the MMP and GOMP, a stage-determined matching pursuit (SdMP) was proposed in [112] that aims at selecting more than one index per iteration that surpass a carefully designed threshold. A small difference compared to MMP and GOMP is that the StMP adds a pruning step after the end of some latter iterations (after satisfying a certain sparsity level condition) in order to refine the selection. Finally, approximate message passing algorithm (AMP), which combines the thresholding methods with the message passing ones, performs well for highly structured measurement matrices [93].

*A Sparse Formulation of the mmWave Channel Estimation Problem:* The mmWave system model is described in equation (13). In what follows, some indices will be omitted for simplicity. Let us consider the received signal at $Q$ successive instants when the same precoder, $\mathbf{F}$, and the same combiner, $\mathbf{W}$, are employed. To exploit the sparse nature of the channel, the concatenated matrix is vectorized, the $Q \times D_T$ resultant vector, $\mathbf{y}_v$, can then be written as [71], [90],

$$\mathbf{y}_v = \sqrt{P}\mathbf{F}^T\mathbf{A}^*_{\mathrm{B,D}}\mathbf{Z}_{\mathrm{B}} \otimes \mathbf{W}^H\mathbf{A}^*_{\mathrm{T,D}}\mathbf{Z}_{\mathrm{T}} + \mathbf{n}_v, \qquad (18)$$

where the $N_{\mathrm{G}} \times 1$ sparse vectors, $\mathbf{Z}_{\mathrm{B}}$ and $\mathbf{Z}_{\mathrm{T}}$, have non-zero elements that correspond to the actual AoDs and AoAs. $\mathbf{A}_{\mathrm{B,D}}$ and $\mathbf{A}_{\mathrm{T,D}}$ are, respectively, the $N_{\mathrm{B}} \times N_{\mathrm{G}}$ and $N_{\mathrm{T}} \times N_{\mathrm{G}}$ beamforming dictionary matrices at the BS and MT. Each dictionary consists of column vectors which represent the complex antenna steering vectors corresponding to the $N_{\mathrm{G}}$ spatially quantized directions, i.e. it is assumed that each direction is defined by an angle which is taken from $\{0, \frac{2\pi}{N_{\mathrm{G}}}, \cdots, \frac{2\pi(N_{\mathrm{G}}-1)}{N_{\mathrm{G}}}\}$. Equation (18) introduces a sparse formulation of this problem by employing a compression matrix which can be expressed as a function of beamforming dictionaries, precoder and combiner matrices [71], [90]. This allows to estimate the channel by detecting and estimating the non-zero elements of $\mathbf{Z}_{\mathrm{B}}$ and $\mathbf{Z}_{\mathrm{T}}$ with a small number of measurements. The CS tools will be able to guarantee that if only the compression matrix is well-designed which in turn requires an efficient design of the precoder and the combiner.

Hence, the estimation of mmWave channels is enabled by reformulating the matrix system model into a sparse problem, before compressing the sparse matrices into reduced-size ones, and finally employing the appropriate CS reconstruction method. Basically, CS-based methods have a significant improvement over most traditional ones, a conclusion made in almost all recent studies on mmWave channel estimation [18]. Such conclusion motivated the practical usage of CS solutions for estimating mmWave channels as will be shown in the upcoming sections [69], [71], [74], [88], [104], [113]–[127].

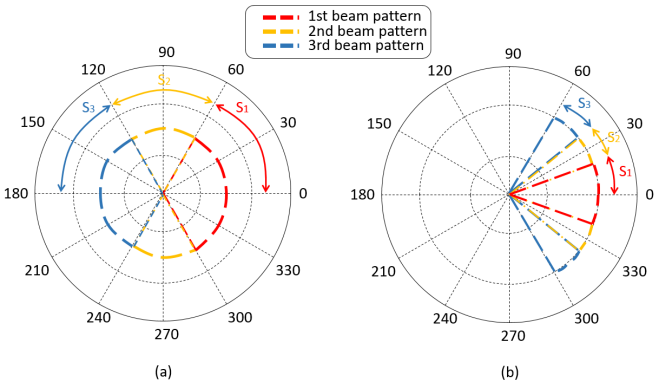


Figure 4. An example of the beam patterns adopted in the first (a) and second (b) stages in [71] when $K = 3$, where $S_k, k \in \{1, \ldots, K\}$ denotes the sub-ranges in each stage.

## V. Channel Estimation Techniques for Hybrid Architecture Systems

For the sake of attaining more precoding gains as well as to be able to precode simultaneously multiple data streams, numerous studies have been proposed to split the precoding process into analog and digital domains [60], [71]. Moreover, to overcome the limitations of analog-only beamforming mmWave systems, constrained by the analog phase shifters amplitude which has to be constant, and by the potentially low-resolution signal phase control, several works have adopted the joint analog-digital hybrid architecture. Some channel estimation methods with this hybrid architecture have been proposed taking into account the aforementioned constraints. Most of these works assume a frequency-flat narrowband mmWave channel model, [62], [71], [104], [128]–[132]. However, several papers have been proposed focusing on the frequency-selective channel case [119]–[121]. In the following paragraphs, we will first present the different approaches for mmWave channel estimation with hybrid architecture when the system is narrowband, before presenting the research works under the frequency-selective channel assumption.

### A. Techniques for Narrowband Systems

Different approaches are employed to estimate the frequency-flat mmWave channel including divide-and-conquer, ping-pong, mode-by-mode approaches and many others. These approaches are explained below in addition to other methods, and they are listed in Table II with their respective references. Furthermore, Table III refers to the definition of the parameters used in the upcoming sections, note that the indices B, T stand for the BS and MT, respectively.

This work is licensed under a Creative Commons Attribution 4.0 License. For more information, see https://creativecommons.org/licenses/by/4.0/.

This article has been accepted for publication in a future issue of this journal, but has not been fully edited. Content may change prior to final publication. Citation information: DOI 10.1109/OJCOMS.2020.3015394, IEEE Open Journal of the Communications Society



Table II
CHANNEL ESTIMATION ALGORITHMS FOR NARROWBAND HYBRID MMWAVE SYSTEMS.

| Reference | Year | Approach | Scenario | UL/DL | 2D/3D | Complexity | Description |
|---|---|---|---|---|---|---|---|
| Alkhateeb *et al.* [71] | 2014 | Divide-and-conquer | Single-user | DL | 2D | $\mathcal{O}(KL^2\lceil KL/M\rceil \log_K(N_G/L))$ | OMP, LSE |
| Lee *et al.* [104] | 2014 | Open-loop | Single-user | Not specified | 2D | $\mathcal{O}(LK_B K_T {N_G}^2)$ | OMP, MG-OMP, LSE |
| He *et al.* [133] | 2014 | Mode-by-mode | Single-user | UL/DL | 2D | Not specified | A temporally correlated NLOS channel, based on the TDD correlation statistics |
| Schniter *et al.* [88] | 2014 | Aperture shaping | Not specified | Not specified | 2D | Not specified | LASSO, LMMSE |
| Alkhateeb *et al.* [113] | 2014 | Ping-ping | Single-user | UL/DL | 2D | $\mathcal{O}(KL^2 N_B \log_K(N_G/L))$ | OMP, no feedback is needed |
| Payami *et al.* [134] | 2015 | Ping-pong | Single-user | Not specified | 2D | $\lceil N/M\rceil$ measurements to scan all $N$ directions | The training time doesn't scale with the number of multi-path components |
| Kokshoorn *et al.* [135] | 2015 | Overlapped beam patterns | Single-user | Not specified | 2D | $\frac{K^2}{\log_2^2(K+1)}$ reduction compared to [71] | MRC, used to track fast changing channels |
| Peng *et al.* [114] | 2015 | AAVE | Single-user | UL | 2D | $2M$ time slots | CS-based technique, enhances the angular estimation resolution |
| Montagner *et al.* [136] | 2015 | 2D DFT | Single-user | Not specified | 2D | $\lceil\frac{N_{D_T}}{M_T}\rceil\lceil\frac{N_{D_R}}{M_B}\rceil M_B$ time slots | DFT, iterative cancellation method |
| Mendez-rial *et al.* [115] | 2015 | Switches | Single-user | DL | 2D | Not specified | OMP, M-OMP |
| Chiang *et al.* [116] | 2016 | SVD avoidance | Single-user | Not specified | Not specified | Not specified | OMP, it exploits the orthogonality between the array propagation vectors |
| Lu *et al.* [137] | 2016 | Adaptive DFT | Single-user | DL | 2D | $\lceil\frac{N_{D_T}}{M_T}\rceil\lceil\frac{N_{D_R}}{M_B}\rceil M_B$ time slots | DFT, a feedback is adopted to improve the accuracy |
| Han *et al.* [117] | 2016 | Two-stage asymmetric | Multi-user | DL | 2D | Not specified | Exhaustive search, CS |
| Park *et al.* [118] | 2016 | Spatial covariance | Single-user | UL | Not specified | Not specified | OMP, S-OMP, C-OMP, DS-OMP, DC-OMP |
| Zhou *et al.* [138] | 2016 | CANDE-COMP/PARAFAC (CP) | Multi-user | UL | 2D | $\mathcal{O}(N_{G1}^2 N_{G2}^2 + T'TM_B)$ | CP, referred to as tensor rank decomposition |
| Guo *et al.* [139] | 2017 | 2D beamspace MUSIC | Single-user | Not specified | 2D | The main complexity comes from (i) the eigenvalue decomposition: $\mathcal{O}(M_B^3 M_T^3)$ (ii) the grid search: $\mathcal{O}(N_{G2}N_{G1}M_B^2M_T^2)$ | MUSIC, LSE, it exploits the large-scale fading property of path directions |
| Guo *et al.* [140] | 2019 | Dimension-deficient | Single-user | UL | 2D | $\mathcal{O}(MN_B(N_T L)^3)$ | CoSaMP, it reduces the influence of accidental errors |

*Divide-and-conquer approach:* In [71] a low-complexity adaptive channel estimation algorithm has been proposed for narrowband mmWave channel with large antenna arrays and a few number of RF units at both the BS and MT sides. The authors assumed that the amplitude of phase shifters is constant, and that the phases are quantized. The algorithm *divides* the estimation process into several stages as shown in figure 4. At each stage, the AoAs/AoDs angular ranges are divided into $K$ non-overlapped angular sub-ranges, $K$ beam patterns are used to send the pilot signal and $K$ beam patterns are used to combine the signal at the receiver. So each beam pattern at the transmitter is combined by $K$ beam patterns at the receiver, as a result, each stage needs $K^2$ time slots to span all the combinations of transmit-receive beam patterns. The beam patterns are taken from a predefined codebook designed and proposed by the authors. The process is then continued by calculating the magnitudes of the $K^2$ received signals to determine or *conquer* the next AoA/AoD angular sub-range for the next stage. At each stage, the process pursues the same way as in the previous stage, in which it divides the chosen AoD sub-range at the transmitter and AoA sub-range at the receiver into $K$ sub-ranges. It proceeds this way until it achieves the desired AoA/AoD resolution. This algorithm, initially proposed for single-path and multi-path cases, needs $K^2\lceil\log_K(max(N_B, N_T))\rceil$ time slots for each channel path. Such algorithm is not fast enough to track the rapid variations of mmWave channels which could be a major drawback. Moreover, this algorithm requires an exclusive feedback channel.

Table III
PARAMETERS GUIDE FOR METHODS PRESENTED IN THE PAPER

| Parameters sheet | |
|---|---|
| $N$ | The number of antennas |
| $M$ | The number of RF chains |
| $L$ | The number of channel paths |
| $K$ | The number of beam patterns or beamforming vectors |
| $n, k$ | $n$ is the size of a sparse vector and $k$ is its sparsity |
| $N_G, N_{G,1}, N_{G,2}$ | The numbers of points of the uniform grids |
| $K_s$ | The number of subcarriers |
| $K_p$ | A reduced number of subcarriers |
| $D$ | The delay spread of the channel |
| $T, T'$ | The number of frames and sub-frames, respectively. |
| $A_v$ | The number of virtual antennas |
| $j$ | The index of a current iteration in an algorithm |
| $N_{TS}$ | The training sequence length |
| $N_{D_T}, M_{D_B}$ | Suitable integers depend on $N_{TS}$ |
| $Q$ | The number of snapshots or time instants |
| $N_f$ | The number of non-overlapping antenna subsets |

*Ping-pong approaches:* Based on the same codebook design, the authors appended their work in [71] by proposing another estimation algorithm that doesn't need feedback in [113]. The developed algorithm uses *ping-pong* iterations, which requires a complexity of $\mathcal{O}(KL^2N_B \log_K(N_G/L))$, to acquire the channel parameters, where the AoAs, and AoDs are taken from a uniform grid of $N_G$ points. In [134] a two-stage algorithm for single-user (SU) channel estimation is presented as well as a codebook design which is similar to that in [113]. The algorithm is characterized by a two-stage handshaking between the transmitter and the receiver. During the first stage, the transmitter uses one transmit antenna

This work is licensed under a Creative Commons Attribution 4.0 License. For more information, see https://creativecommons.org/licenses/by/4.0/.

This article has been accepted for publication in a future issue of this journal, but has not been fully edited. Content may change prior to final publication. Citation information: DOI 10.1109/OJCOMS.2020.3015394, IEEE Open Journal of the Communications Society



to send an omni-directional signal and correspondingly the receiver senses and scans its multiple directions to detect the AoA angles, subsequently the roles are exchanged at the second stage such that the receiver sends a pilot signal at the detected angles only. The two-stage estimation algorithm is illustrated in figure 5. It needs $\lceil N/M \rceil$ measurements to scan all $N$ required directions, where $M$ is the number of the RF chains in the system. Moreover, its training time doesn't scale with the number of multi-path components, unlike the channel estimation method in [113].

*Overlapped beam patterns approach:* [135] outlined a fast channel estimation algorithm by proposing the *overlapped beam patterns* estimation concept. This concept reduces the time slots needed to estimate the channel by $\frac{K^2}{log_2^2(K+1)}$ compared to [71], with a slight degradation in performance. This small sacrifice in degradation can be accepted when tracking fast changing channels is required. Indeed, the concept is to use a smaller number of overlapped beam patterns for the same number of sub-ranges to estimate the channel, instead of assigning one beam pattern for each sub-range as in [71] in which the number of beam patterns should be equal to the number of sub-ranges. The algorithm is illustrated in figure 6.

*Open-loop approach:* An *open-loop* channel estimation technique that doesn't need a feedback loop was proposed in [104]. The algorithm is provided for an SU mmWave system, and is based on CS techniques. As for many channel estimation algorithms, the authors used the OMP and least-squares estimation (LSE) techniques to perform the estimation of the AoAs/AoDs and gains, respectively. However, they also proposed the adaptive MG-OMP, this new version of OMP enhances the estimates of AoAs/AoDs by refining these estimates just around the regions where the AoAs/AoDs are present which reduces MG-OMP complexity over OMP. Through their computer simulations, the authors showed that CS techniques, OMP and MG-OMP, outperforms the LSE ones. In addition, the complexity reduction gained by the MG-OMP was estimated.

*Mode-by-mode approach:* Another scheme was proposed in [133] to estimate a temporally correlated NLOS mmWave MIMO channel. The authors, first modified the parametric channel model to an evolution temporally correlated MIMO channel model to successfully track the channel variations. The system is based on the TDD correlation statistics and it exploits the reciprocity of the channel. The proposed algorithm updates each column of the analog precoder and combiner, this approach is called the *mode-by-mode* approach, in which each mode represents one column of the analog precoder and combiner. For each mode, a codebook is built using a group of rotation matrices that rotate the previous mode to reconstruct the new mode, then the algorithm chooses the codeword that maximizes the received power. The digital precoder and combiner are then constructed using conventional pilot-aided estimation of the effective channel.

*Aperture shaping approach:* In [88], P. Schniter and A. Sayeed proposed a technique termed as *aperture shaping* to enhance the sparsity of the virtual MIMO channel. Briefly, aperture shaping is performed by applying a fixed gain at each antenna at both the TX and RX. The shaping coefficients are optimised to maximize the signal-to-interference ratio. In addition, they implemented a mmWave system that uses modulation and demodulation techniques based on fast Fourier transform (FFT) to further expose the channel sparsity. Finally, waterfilling technique and Lanczos algorithm were employed to design spectrally efficient precoding and decoding. They solved the sparsity problem using LASSO [102], where it was shown that their procedure approaches the perfect-CSI capacity for a mmWave system.

*AAVE approach:* Based on the same assumptions as in [71], the authors in [114] proposed a new concept called antenna array with virtual elements *(AAVE)*, that extends the real antenna arrays at both the transmitter and receiver to a new one by appending some $A_v$ virtual antennas without affecting the physical array. The idea behind AAVE is to add some virtual antennas to the real physical antennas at both the BS and MT, in order to enhance the angular estimation resolution. However, the scheme assures that no data is sent over the virtual antennas to guarantee that no physical change has been introduced to the antenna arrays. Based on AAVE, [114] develops a CS angle estimation method with less overhead and delay than [71]. The proposed method with AAVE can obtain a resolution of $\mathcal{O}(1/A_v)$ which is better than $\mathcal{O}(1/N_{\mathrm{G}})$ in [71], [135], [141].

*2D DFT approach:* In [136], a mmWave channel estimation method was proposed based on the *2D DFT*. The estimation of the channel parameters is done using the iterative cancellation method. In detail, the approach estimates the channel parameters for each path using the DFT samples, after cancelling the previous estimated parameters in each iteration. This technique requires a training sequence of $N_{\mathrm{TS}} = \lceil \frac{N_{D_T}}{M_{\mathrm{T}}} \rceil \lceil \frac{N_{D_B}}{M_{\mathrm{B}}} \rceil M_{\mathrm{B}}$ time slots, where $N_{\mathrm{D}}$ and $M_{\mathrm{D}}$ are two suitable integer parameters to be chosen depending on the length $N_{\mathrm{TS}}$ of the training sequence. The method showed low complexity and performed close to a known channel system. Another channel estimation algorithm for a DL SU mmWave system was proposed in [137] based on the *DFT* algorithm in [136]. The algorithm uses exactly the same DFT technique provided in [136], while adopting a feedback to the BS to improve the estimation accuracy. The algorithm is illustrated as follows: First, the BS sends its training sequence to the MT, the MT estimates the channel using the DFT technique, and determines if the estimation is accurate based on an adjustable threshold. Second, the MT returns *YES* or *NO* to the BS depending on the accuracy of its estimation. Third, the BS readjusts the length of the training sequence *adaptively* according to the feedback.

*Switches approach; SVD avoidance approach:* In [115], the authors proposed a new hybrid architecture for a DL SU mmWave system using *switches* as an alternative for phase shifters, to reduce cost, complexity and power consumption, especially at MTs where these parameters are crucial. Figure 7 depicts the proposed hybrid architecture which is slightly different from the aforementioned one as it was presented in figure 3(b). A new CS-based channel estimation algorithm was also developed. A multiple measurement vector OMP (M-OMP) in [142] was considered instead of the single measurement vector OMP. Phase shifters architecture versus switches architecture were compared, the results showed a slight better

This work is licensed under a Creative Commons Attribution 4.0 License. For more information, see https://creativecommons.org/licenses/by/4.0/.

This article has been accepted for publication in a future issue of this journal, but has not been fully edited. Content may change prior to final publication. Citation information: DOI 10.1109/OJCOMS.2020.3015394, IEEE Open Journal of the Communications Society



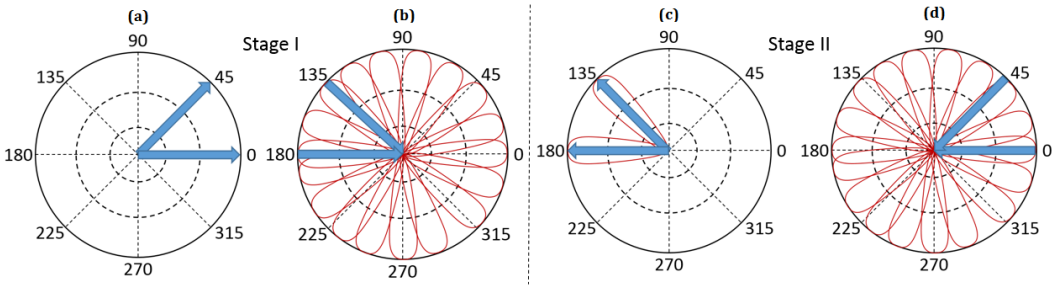


Figure 5. Illustration of the two-stage estimation algorithm in [134], the blue colored arrows represent the AoA/s and AoD/s at the BS and MT; (a) the BS sends an omni-directional signal, (b) the MT scans the directions, (c) the MT sends through its AoDs, (d) the BS scans the directions

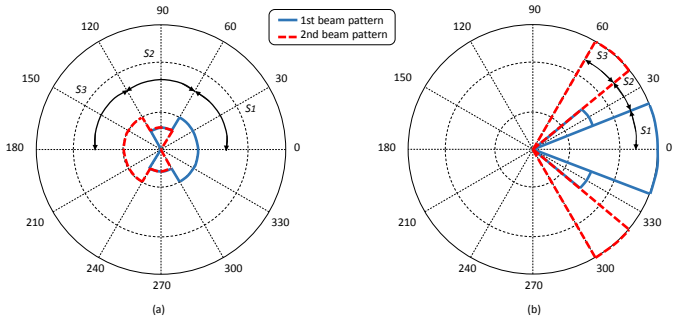


Figure 6. The overlapped beam patterns adopted in the first (a) and second (b) stages when $K = 3$

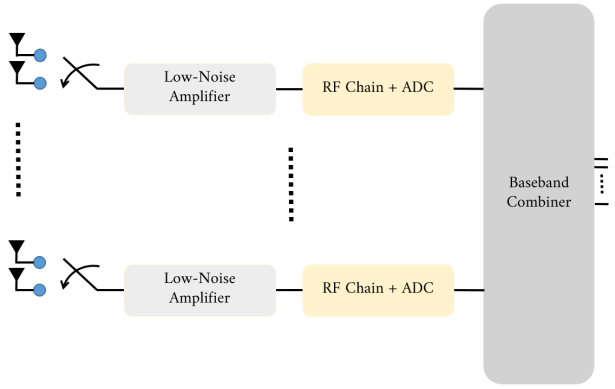


Figure 7. Hybrid mmWave MT architecture implementing switches instead of phase shifters

performance of the architecture implementing switches over phase shifters one. A modified version of the aforementioned algorithm was proposed in [116] for an SU mmWave system. The authors intended to reduce the computational complexity and feedback overhead to the TX. The algorithm is also based on the OMP, but unlike to [115] it *avoids* the computation of the channel *SVD* at the RX by exploiting the orthogonality between the array propagation vectors. In contrast to [115], where the whole reconstructed precoder is sent back to the TX through the feedback link, the algorithm in [116] diminishes the feedback overhead, since it aims to reconstruct the precoder at the TX, after obtaining the codebook indices through the feedback link.

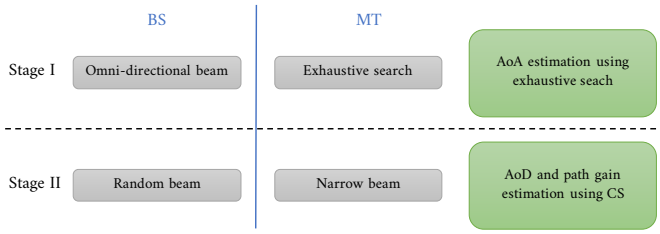


Figure 8. The two-stage asymmetric estimation approach in [117]

*Two-stage asymmetric approach:* An asymmetric channel estimation approach was proposed in [117] for a DL multi-user (MU) mmWave system. The MU system is characterized by a hybrid BS and analog-only beamforming at the MTs with one RF chain for each MT. The proposed algorithm is a *two-stage asymmetric* approach, an exhaustive search stage, followed by a CS estimation stage. At the first phase, the BS sends the omni-directional training signals to the MTs, the MTs search in exhaustive manner for the best combining vectors to find the AoA. Following the first phase, a second phase of CS estimation is performed, where the MTs fix their receiving beams to the best ones found at the first phase, while utilizing CS tools to estimate their channel parameters. The two-stage algorithm is depicted in figure 8.

*Spatial covariance approach:* In [118], a channel estimation algorithms based on estimating the *spatial covariance* for a TDD UL SU mmWave channel were proposed. Unlike the two-step approach, where first it is needed to estimate the channel, followed by a second step of channel covariance calculation. The authors proposed to estimate the channel covariance directly, and without estimating the channel explicitly. To overcome the need of estimating the channel explicitly, the authors exploited the Hermitian property of the spatial covariance channel matrix. A sparse Hermitian matrix is shown in figure 9(c). Furthemore, the authors designed the covariance OMP (C-OMP) algorithm, which is based on the OMP and simultaneous OMP (S-OMP), to exploit this property and to estimate the covariance of the channel. C-OMP employs a quadratic form in its covariance calculations unlike OMP and S-OMP where a linear form is used. As known, for a perfect recovery using CS techniques, many measurements are required especially for time-varying channels. Accordingly, the authors also proposed dynamic S-OMP (DS-OMP), which was

This work is licensed under a Creative Commons Attribution 4.0 License. For more information, see https://creativecommons.org/licenses/by/4.0/.

This article has been accepted for publication in a future issue of this journal, but has not been fully edited. Content may change prior to final publication. Citation information: DOI 10.1109/OJCOMS.2020.3015394, IEEE Open Journal of the Communications Society



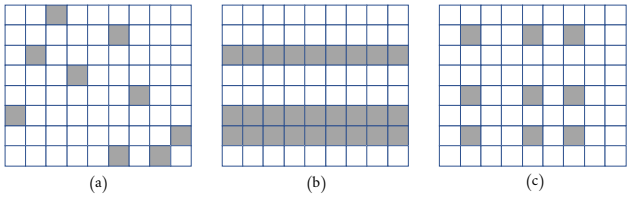


Figure 9. Different sparse matrix types (a) Unstructured sparse matrix (b) Sparse rows matrix (c) Sparse Hermitian matrix.

inspired by S-OMP, to mitigate the number of measurements, similarly, dynamic C-OMP (DC-OMP) was introduced. Both DS-OMP and DC-OMP can be applied to a time-varying analog combining matrix in a time-varying channel.

*Over-complete dictionary approach:* Another channel estimation algorithm for a fully-connected UL SU mmWave system has been developed in [140]. The authors described the channel estimation problem by *dimension-deficient* which results from the fact that the number of RF chains is a lot smaller than the number of antennas, hence the received signal does not contain full CSI. The authors treated this issue by adopting an adaptive over-complete dictionary, then by estimating the channel parameters using CoSaMP which improves the OMP technique by reducing the influence of accidental errors. The proposed algorithm showed more robustness against noise, better performance compared with non-adaptive CS techniques, with spectral efficiency close to perfect CSI.

*Other approaches:* Some works tried to compete with CS algorithms in estimating the mmWave channel. Based on a technique termed *CANDECOMP/PARAFAC* (CP) decomposition, an interesting method was carried out in [138] and was also compared to some CS techniques. In this regard, the UL MU mmWave channel can be estimated by means of the CP decomposition method. This procedure also referred to as tensor rank decomposition, can be viewed as a generalisation of the matrix singular value decomposition to tensors. Please refer to [143] for more details. The authors stated that the CP method can be advantageous when compared to CS techniques in terms of computational complexity due to the utilization of tensors. In addition, while it is somewhat troublesome to examine the right recovery condition for generic dictionaries, this is not the case for the CP method, hence it is more easier to analyze and find the exact size of training overhead. Moreover, unlike CS methods, the CP doesn't require the quantization of the continuous parameter space, consequently, no grid quantization errors. The overall computational complexity of the proposed CP method was shown to be $\mathcal{O}(N_{G1}^2 N_{G2}^2 + T'TM_B)$, where $T$ and $T'$ are respectively the number of frames and sub-frames (each frame is divided into a number of sub-frames), and $N_{\mathrm{G2}}$ and $N_{\mathrm{G1}}$ are respectively the search grid sizes within the considered beamforming sectors. Another contribution to estimate an SU mmWave channel was achieved in [139] based on a 2D beamspace *multiple signal classification* (MUSIC) method. The MUSIC method is used to estimate the path directions while the LSE one estimates the path gains. The suggested algorithm reduces the computational overhead by exploiting the large-scale fading property of the path directions which are believed to remain unchanged for each frame according to the measurement results obtained in [29]. Hence the costly computation of path directions is executed only once per each frame. The main computational complexity analysis of the algorithm brings out two major tasks (i) the eigenvalue decomposition whose complexity is $\mathcal{O}(M_{\mathrm{B}}^3 M_{\mathrm{T}}^3)$ (ii) the grid search whose complexity is $\mathcal{O}(N_{\mathrm{G2}} N_{\mathrm{G1}} M_{\mathrm{B}}^2 M_{\mathrm{T}}^2)$.

### B. Techniques for Wideband Systems

Most of the work done on mmWave channels estimation assumed the narrowband case. Such assumption was found to be not realistic for aforementioned channels, but was considered as a first step in the development of mmWave channel estimation. MmWave channels are wideband channels in reality, and to be useful, channel estimation algorithms have to take this into consideration. Recently, some works have been proposed to estimate the frequency-selective channels for mmWave hybrid systems, we review these works in the following. Table IV provides a list of these research works.

*Time-domain approach:* In [119] a time-domain channel estimation algorithm was proposed for both single- and multi-user fully-connected hybrid single-carrier mmWave systems. The authors had taken into account the bandlimitting filter and the time required to reconfigure RF circuits. The proposed algorithm is based on CS to estimate the AoAs/AoDs, and on the LSE or the minimum mean square error (MMSE) to estimate the path gains. Simulation results showed that the proposed algorithm provides low estimation error using small training overhead, but the main drawback of this algorithm lies into its complexity.

*Frequency-domain approaches:* In [122], two frequency-domain channel estimation algorithms for a fully-connected OFDM mmWave system were proposed based on the S-OMP method [145] and tested on real frequency-selective channel models. The proposed algorithms provide a trade-off between complexity and achievable rate, and consider the effects of the bandlimitting filter and the time required to reconfigure RF circuits. The first algorithm termed as the simultaneous weighted OMP (SW-OMP) provides the best performance compared to the second one since it exploits the information on the support coming from every subcarrier of the OFDM system. While the second algorithm termed as subcarrier selection SW-OMP + thresholding (SS-SW-OMP+Th) aims to exploit information from a reduced number of subcarriers, hence it provides a lower complexity compared to SW-OMP. Both algorithms achieve the Cramer-Rao lower bound. Comparisons were done for the proposed algorithms and other frequency-selective mmWave channel estimation algorithms including structured sparsity adaptive matching pursuit (SSAMP) [146] and distributed grid matching pursuit (DGMP) [123]. The simulation results show a very good performance of the proposed algorithms.

Another frequency-domain algorithm was developed in [121], for a fully-connected OFDM mmWave system. The algorithm was compared with the time-domain algorithm proposed in [119], where it provides the same estimation error

This work is licensed under a Creative Commons Attribution 4.0 License. For more information, see https://creativecommons.org/licenses/by/4.0/.

This article has been accepted for publication in a future issue of this journal, but has not been fully edited. Content may change prior to final publication. Citation information: DOI 10.1109/OJCOMS.2020.3015394, IEEE Open Journal of the Communications Society



Table IV
CHANNEL ESTIMATION ALGORITHMS FOR WIDEBAND HYBRID MMWAVE SYSTEMS.

| Reference | Year | Scenario | UL/DL | 2D/3D | Complexity | Description |
|---|---|---|---|---|---|---|
| Venugopal *et al.* [119] | 2017 | Single-user or multi-user | DL | 2D | Not specified | CS, LSE, high complexity |
| Venugopal *et al.* [120] | 2017 | Single-user or multi-user | Not specified | 2D or 3D | Not specified | OMP, DGMP, LSE, MMSE, SC-FDE or OFDM are considered |
| Rodriguez-fernandez *et al.* [121] | 2017 | Single-user | Not specified | 2D | Not specified | OMP, MSE, LSE, exploits the common support between the subcarriers to reduce complexity |
| Rodriguez-fernandez *et al.* [122] | 2018 | Not specified | Not specified | 2D | SW-OMP: $\mathcal{O}(M_T T(K_s(N_{G1}N_{G2}-(j-1))))$; SS-SW-OMP+Th: $\mathcal{O}(M_T T(K_p(N_{G1}N_{G2}-(j-1))))$ | SW-OMP, SS-SW-OMP+Th, provides a trade-off between complexity and achievable rate |
| Gao *et al.* [123] | 2016 | Multi-user | UL | 2D | Not specified | DGMP, exploits the angle-domain sparsity of frequency-selective fading channels |
| Zhou *et al.* [144] | 2017 | Multi-user | DL | 2D | $\mathcal{O}(T'TK_s)$ | CP, higher estimation accuracy compared to OMP |
| Araujo *et al.* [124] | 2014 | Single-user | DL | 3D | $\mathcal{O}(\log(N_{\mathrm{B}}))$ | OMP, *search region*, a coarse stage followed by a refinement stage |
| Gonzalez-coma *et al.* [74] | 2018 | Multi-user | UL | 2D | $\mathcal{O}(M_{\mathrm{T}}T(K_s(N_{G1}N_{G2}-(j-1))))$ | SW-OMP |

as the time-domain one, however with a lesser complexity. The authors opted to use OMP and LSE techniques to estimate the sparse channel, and exploited the common support between the subcarriers to gain more reduction in estimation complexity. In addition, they proposed to refine more the estimates using an algorithm they termed as the joint channel estimation + local search (JCE+LS), which is based on minimum square error (MSE) to know whether an improvement of the estimates is needed or not.

In [123], a frequency-domain CS-based UL MU channel estimation algorithm was proposed for OFDM mmWave system. The proposed DGMP algorithm aims to exploit the angle-domain sparsity of frequency-selective fading channels, and solves the problem of the leakage power caused by the continuous AoA/AoD. The simulation results showed a good performance of the proposed algorithm.

Based on the SW-OMP algorithm developed in [122], the authors in [74] proposed a joint UL MU channel estimation method for an OFDM mmWave system. Afterwards, the UL channel estimates and the reciprocity of TDD scheme were exploited to jointly design the precoders and combiners in the DL.

*Two-stage approach:* A two-stage channel estimation algorithm has been proposed in [124] for an indoor SU DL mmWave system, implementing FDD and OFDM, and operating at 60 GHz. The estimation algorithm is based on two stages, a coarse stage followed by an amelioration stage. The first stage of the algorithm is performed based on the OMP CS technique, which estimates the parameters of the channel coarsely. Subsequently, the second stage is carried out to refine the estimates based on the maximization of the energy of the received signal and using the so-called *search region* algorithm as described in the paper. The proposed method can achieve a low pilot overhead of $\mathcal{O}(\log N_{\mathrm{B}})$ compared to the traditional LSE that requires a length of $\mathcal{O}(N_{\mathrm{B}})$, and shows a quite well performance.

*Other approaches:* The authors in [120] developed channel estimation algorithms in the frequency-domain, in the time-domain, as well as in the combined time/frequency domain. Both single- and multi-user fully-connected hybrid mmWave systems implementing either single carrier-frequency domain equalization (SC-FDE) or OFDM are considered. The estimators are based on CS, where OMP is the dominant technique used to estimate AoAs/AoDs, while LSE is used to estimate channel gains, whether for the time-domain or the frequency-domain. However, for the combined time/frequency domain, OMP or DGMP [123] are used to estimate AoAs/AoDs, and LSE or MMSE to recover the gains. The results showed a good error performance with low overhead, and a further reduction in complexity offered by the combined time/frequency algorithm.

Similarly to the CANDECOMP/PARAFAC narrowband mmWave channel estimation algorithm proposed in [138], an MU DL channel estimation technique for OFDM mmWave systems was proposed in [144]. The authors developed the Cramer-Rao bound results to describe the best asymptotically achievable performance of the algorithm, then they compared the proposed algorithm to the OMP method, where it was shown to provide a complexity similar to the OMP method, but with higher estimation accuracy.

### *Conclusions*

The usage of analog-only beamforming for channel estimation in mmWave systems is constrained by many limitations, which can be avoided using the hybrid architecture. In this section we have seen different channnel estimation techniques for both narrowband and wideband hybrid mmWave systems. It can be said that there exist plenty of research works on channel estimation for the narrowband case, while only few papers have been proposed for the wideband one. It is known that mmWave channels are wideband in nature, hence some further future steps have to be taken in this regard. Clearly the aim of most of the work that has been delivered so far for hybrid architecture was for 2D channel estimation, this work should be extended to the 3D case also.

## VI. CHANNEL ESTIMATION TECHNIQUES FOR SYSTEMS WITH LENS ANTENNA ARRAY

In this section, we focus on the channel estimation problem for the mmWave massive MIMO systems with lens antenna

This work is licensed under a Creative Commons Attribution 4.0 License. For more information, see https://creativecommons.org/licenses/by/4.0/.

This article has been accepted for publication in a future issue of this journal, but has not been fully edited. Content may change prior to final publication. Citation information: DOI 10.1109/OJCOMS.2020.3015394, IEEE Open Journal of the Communications Society



array. Under this assumption, the conventional channel estimation techniques for fully-digital architectures are obviously not applicable since the number of RF chains is limited. In addition, the above presented channel estimation techniques for hybrid architectures are also unsuitable for lens antenna arrays mmWave systems for mainly two reasons. The first one is related to the simple switching network employed at the BS and/or MT to simplify the analog beamformers of the hybrid schemes where the RF chains are connected with all the antennas with phase shifters and power splitters. The simplicity of the analog precoding/combining circuits in mmWave systems with lens antenna array comes on the price of stronger constraint when compared to the constant modulus one of the phase shifters network [83], [86]. Secondly, lens antenna arrays are able to focus the signal with distinct AoAs onto different antennas, contrary to the ULPA where the energy is distributed uniformly on all the antennas of the array. That is why several research works tries to develop tailored channel estimation techniques for mmWave systems with lens antenna array in order to exploit its focusing-energy feature [83], [86], [147]–[151].

The authors in [149] considered a narrowband model for the UL MU mmWave channel consisting of a massive-MIMO BS and $U$ single-antenna MTs. The beamspace channel is estimated via a sparsity mask detection method where a beam training procedure between the BS and the $U$ users is first employed to determine which beams with large power are simultaneously used by the BS; this defines the sparsity mask [152], [153]. Then, the dimension of the beamspace channel is reduced, and conventional algorithms are used to estimate the dimension-reduced channel. However, the BS overhead is still proportional to the dimension of its antenna array, which is large.

In [150], a BS equipped with a 2D lens array and a zero forcing (ZF) precoder, communicating with $U$ single-antenna MTs is considered. The beams that will be employed by the BS during the data transmission are identified via a beam selection technique. This research work applied three different criteria to select beams, namely the magnitude of the path [152], the signal-to-interference-plus-noise ratio (SINR) at the MT side [154], the capacity of the full system [155]. The authors demonstrated that the maximum magnitude beam selection scheme can achieve near-optimal performances in both line-of-sight (LOS) and multi-path scenarios. The complexity and the overhead of the above presented methods can be reduced by utilizing CS tools [94], [156], [157] which can further exploit the sparsity of beamspace channel.

*Support-Detection-based Channel Estimation:* In [83], the beamspace channel estimation problem in a TDD system with lens antenna array was investigated. A mmWave massive MIMO BS equipped with $N_{\mathbf{B}}$ antennas and $M_{\mathbf{B}}$ RF chains communicates simultaneously with $U$ single-antenna users. Under the channel reciprocity assumption, the authors proposed to estimate the uplink channel which is just a transposition of the downlink one. They adopted the DFT model to describe the channel, i.e. the lens antenna array plays the role of a spatial DFT matrix which contains the array steering vectors of different orthogonal directions. CS tools were used to propose a support detection (SD)-based beamspace channel estimation with low pilot overhead. Before that a strategy for pilot transmission and adaptive selection network was designed. Thereafter, we will briefly present the three phases of this channel estimation method.

- Pilot Transmission : Known mutually orthogonal pilot sequences are transmitted by the $U$ users to the BS over a certain duration lesser than the channel coherence time such as the beamspace channel remains unchanged during its estimation time.
- Adaptive selecting network : During the pilot transmission, the BS combines the received UL signal via an adaptive selecting network which consists of a small number of 1-bit phase shifters (equivalent to switches in terms of simplicity and energy consumption) to efficiently measure the beamspace channel. CS tools were employed to design a Bernoulli random matrix adaptive combiner such that the required recovery accuracy is guaranteed. The application of the proposed adaptive selecting network makes it possible to formulate the beamspace channel estimation problem as a sparse recovery problem, which significantly reduces the number of required pilot symbols.
- SD-based channel estimation scheme : The channel estimation problem is decomposed into a series of sub-problems where only one sparse channel component is considered for each sub-problem. The idea is to iteratively detect the support (i.e., the index set of non-zero elements) in a sparse vector containing the information of a specific propagation direction at each time. Thereafter, the influence of each channel component is removed from the mmWave beamspace channel, and the support of the next one is detected in a similar way. After completing the detection of the supports of all channel components, the beamspace channel can be estimated with low pilot overhead.

The SD-based channel method can outperform the classical CS algorithms (such as OMP and CoSaMP) which also iteratively estimate all the positions of non-zero elements one by one. The main reason is that the SD-based method only estimates the position of the strongest element, by contrast to the CS algorithms that can try to estimate an element whose power is not strong enough. This becomes more crucial when the transmit power of users is limited. Simulation results confirm that this method provides satisfying performance and low pilot overhead even in the low signal-to-noise ratio (SNR) region.

*Estimation of approximated lens array response:* The research work in [86] studies the mmWave channel estimation problem for a general lens antenna system, i.e. a narrowband or wideband system using a TDD or FDD mode where BS and MT are equipped with lens antenna arrays. The specificity of this paper comes from the fact that it is one of the pioneer works that have adopted the approximated lens array response model as defined in equation (11). The authors assumed that the channel is a quasi-static block-fading one such that the UL/DL channels can be considered constant over some period

This work is licensed under a Creative Commons Attribution 4.0 License. For more information, see https://creativecommons.org/licenses/by/4.0/.

This article has been accepted for publication in a future issue of this journal, but has not been fully edited. Content may change prior to final publication. Citation information: DOI 10.1109/OJCOMS.2020.3015394, IEEE Open Journal of the Communications Society



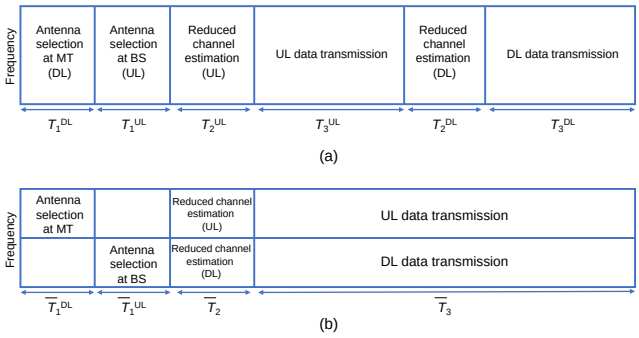


Figure 10. Existing duplexing schemes for mmWave MIMO systems (a) TDD scheme (b) FDD scheme.

and change independently from one period to the next. Each period is divided into three main phases: energy-based antenna selection, reduced MIMO channel estimation and finally data transmission. It is possible to apply this sequence of phases for TDD and FDD schemes as shown in figure 10. Note that the assumption of channel reciprocity was not needed in this paper, and even the authors explained that the path reciprocity assumption is more realist and sufficient to propose an efficient tailored channel estimation method.

In the first phase, the angle-dependent energy focusing of the lens array enables the antenna selection at BS and MT via a simple energy detection and comparison since only a small subset of antennas would receive (steer) significant power from (to) the transmitter (receiver). The antenna selection at the MT is assisted by the BS which first isotropically sends identical training symbols such as those along the few channel paths would be received at the MT. A similar technique is applied to select the BS antennas but this time the MT only sends his signal via its selected antennas which are associated with the most powerful paths of the channel. The employed procedure is illustrated in figure 11.

After antenna selection, the matrices of the UL and DL channel impulse responses, as defined in (2) and (14) respectively, are reduced to the corresponding submatrices associated with the selected antennas. The following phase is to estimate the dimension-reduced matrices which exhibit a highly sparse structure. The UL channel matrix is estimated by sending orthogonal training sequences from each of the selected antennas at the MT. The authors assumed that the received signals of the $L$ paths at the BS are focused on $N_f$ non-overlapping antenna subsets when the angle resolution of the lens antenna array is sufficiently large. Afterwards, a correlation between the received sequences and the training sequence with simple peak searching is employed to estimate the channel gains. This method is efficient since the path-division property of lens antenna array allows to drastically reduce both inter-stream interference within each path and inter-stream interference in other paths. However, the inter-stream interference among paths is much more significant in conventional antenna arrays and that is why the channel impulse response can't be directly estimated.

*Message passing methods:* In [158], the authors investigated the channel estimation problem for a mmWave system with BS and MT equipped with lens antenna arrays. The DFT channel model was adopted such as the channel coefficients are approximately modeled as a Bernoulli-Gaussian distribution. Thanks to the sparse nature of the channel, this research work proposed an iterative estimation method based on two main steps : the LSE and sparse message passing (SMP). The block diagram of this method is presented in figure 12. The SMP is similar to the belief propagation decoding process and its aim is to detect the exact locations of the non-zero entries of the sparse channel matrix or its vectorized version. This step required first to introduce a factor graph representation of the channel such as it is possible to identify two types of nodes : the entries of the received signal vector, and that of a position vector which represents the positions of non-zero coefficients in the channel vector. The extrinsic information on each edge is calculated by the messages on the other edges that are connected with the same node. Then, LSE is applied to estimate the values of the non-zero elements whose positions were previously detected by the SMP. The new channel vector will replace the old input of the SMP step in the next iteration. Of course, this iterative process requires to be initialized via a coarse LSE estimation of the channel vector without taking into consideration its sparsity structure or its degree of sparsity. In addition, it is needed to estimate the sparsity ratio in each iteration. The expectation-maximization (EM) method is employed for that purpose. Actually, the cooperation between the LSE and SMP improves the performance of the estimation at each iteration, until the convergence of the algorithm is reached.

*Channel estimation for 3-D lens systems:* Most existing channel estimation methods are based on the 2D beamspace channel model. However, some papers consider the more general 3D nature of the beamspace [81], [82], [151]. In [151], the authors proposed an adaptive support detection (ASD)-based channel estimation scheme based on decomposing the 3D beamspace channel estimation problem into several sub-problems. For each sub-problem, the support of a sparse channel component is adaptively detected by exploiting the horizontal and vertical sparsity of the 3D beamspace channel. Then, the influence of each detected channel component is successively removed before detecting the support of the following channel component. Finally, the non-zero elements of the 3D beamspace channel is estimated with low-complexity.

The structure of beamspace channel was further analyzed in [81] and it was demonstrated that the dominant entries of its matrix form a dual crossing (DC) shape. The authors proposed an iterative DC-based channel estimation scheme with the aim of refining the selection of dominant entries. This scheme outperforms the existing conventional CS algorithms and the above presented ASD. The performance of this scheme was further improved in [82] by mitigating some iterative steps and consequently the computational complexity was reduced.

*Deep-learning-based methods:* The authors in [159] proposed a deep-learning-based channel estimator for mmWave massive MIMO systems based on learned denoising-based approximate message passing (LDAMP) network. The idea is to exploit a large set of training data to learn the channel structure in order to estimate it. The asymptotic performance of this

This work is licensed under a Creative Commons Attribution 4.0 License. For more information, see https://creativecommons.org/licenses/by/4.0/.

This article has been accepted for publication in a future issue of this journal, but has not been fully edited. Content may change prior to final publication. Citation information: DOI 10.1109/OJCOMS.2020.3015394, IEEE Open Journal of the Communications Society



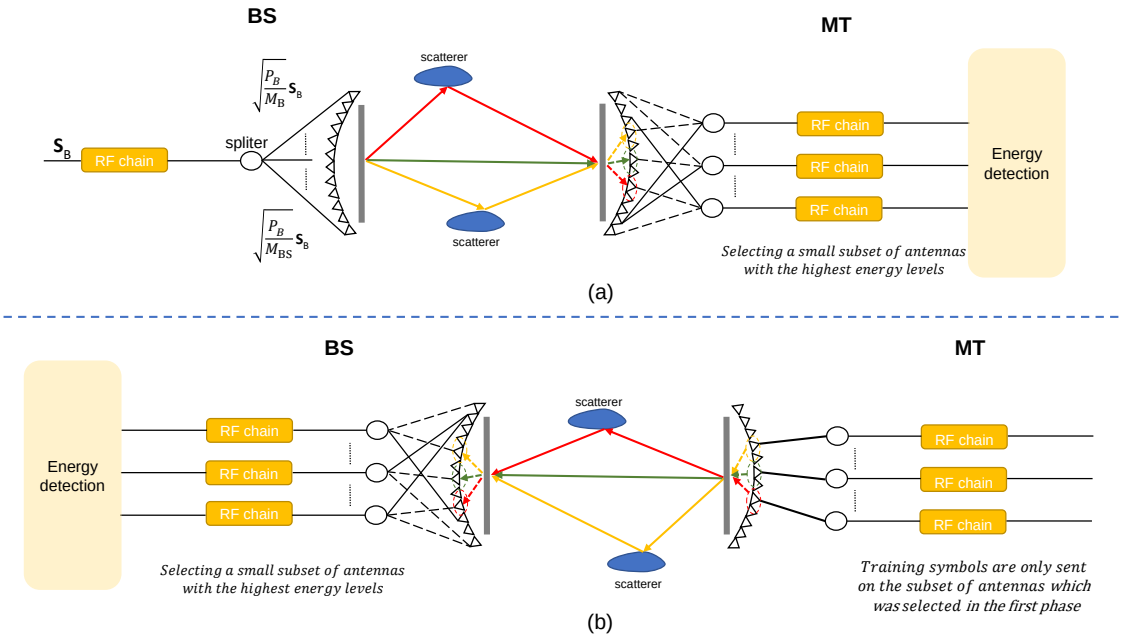


Figure 11. Proposed energy-based antenna selection with lens antenna array (a) Energy-based antenna selection at MT (b) Energy-based antenna selection at BS.

Table V
A COMPARISON AMONG PRINCIPAL CHANNEL ESTIMATION TECHNIQUES WITH LENS ANTENNA ARRAY

| Reference | Year | Scenario | Array Model | Some Assumptions | Multiplexing Mode | 2D/3D | Complexity | Description |
|---|---|---|---|---|---|---|---|---|
| Gao *et al.* [83] | 2017 | $U$ single-antenna users | DFT | Channel reciprocity, narrowband | TDD | 2D | $\mathcal{O}(LQ(N_{\mathrm{B}}+N_f^2))$ | Support detection scheme, only one sparse channel component is considered at each time |
| Yang *et al.* [86] | 2018 | Single-user with lens antenna array | approxi-mate response | Path reciprocity, narrowband or wideband, block-fading channel | TDD or FDD | 2D | $\mathcal{O}(N_f^2)$ | Energy detector, then orthogonal training sequences and a correlation detector |
| Huang *et al.* [158] | 2019 | Single-user with lens antenna array | DFT | Sparsity ratio to be estimated | Not specified | 2D | See section IV. 5 of [158] | Iterative message passing algorithm combined with least-square estimation |
| Gao *et al.* [151] | 2016 | $U$ single-antenna users | DFT | Channel reciprocity, narrowband | TDD | 3D | $\mathcal{O}(LN_f^2)$ | Adaptive support detection then estimation of the non-zero elements |
| Gao *et al.* [84] | 2018 | $U$ single-antenna users | DFT | Channel reciprocity, wideband, beam squint | TDD | 2D | $\mathcal{O}(N_{\mathrm{B}}K_sL+K_sM_{\mathrm{B}}QL+K_sM_{\mathrm{B}}QL^2)$ | Successive support detection, the supports of each path at different frequencies are jointly estimated |
| Ma *et al.* [81] | 2017 | $U$ single-antenna users | DFT | Channel reciprocity, narrowband | Not specified | 3D | $\mathcal{O}(4QN_f+10N_f^2+2N_f)$ | Iterative dual crossing method |
| Cheng *et al.* [82] | 2018 | $U$ single-antenna users | DFT | Channel reciprocity, narrowband | TDD | 3D | $\mathcal{O}(2QN_f+10N_f^2+N_f)$ | Low-complexity iterative dual crossing method |
| He *et al.* [159] | 2018 | Single-user with a single-antenna | DFT | Channel reciprocity, narrowband | Not specified | 3D | Not specified | Learned denoising-based approximate message passing network |

channel estimation scheme was also analyzed. The LDAMP neural network was shown to provide better performance when compared to CS-based methods even when the receiver is equipped with a small number of RF chains. However, deep-learning-based methods have to be trained on real data in order to be capable of performing well when integrated in transceivers.

*Techniques for wideband systems:* The above works did not take into consideration the likely frequency-selective nature of the wideband mmWave channels, and their extension to this case is non-trivial. Indeed, the direction of beams tends to be varying with frequency as the bandwidth and the array size increase, this is called the *beam squint*. Hence, the supports of wideband beamspace channel depend on frequency which complicates their detection. The research work in [84] proposed an efficient successive support detection (SSD)-based beamspace channel estimation scheme which is similar to the classical successive interference cancellation for multi-user detection. For each path component of the wideband beamspace channel, a joint estimation of its supports at different frequencies is conducted before removing its contribution and then estimating the remained path components. Finally, a

This work is licensed under a Creative Commons Attribution 4.0 License. For more information, see https://creativecommons.org/licenses/by/4.0/.

This article has been accepted for publication in a future issue of this journal, but has not been fully edited. Content may change prior to final publication. Citation information: DOI 10.1109/OJCOMS.2020.3015394, IEEE Open Journal of the Communications Society



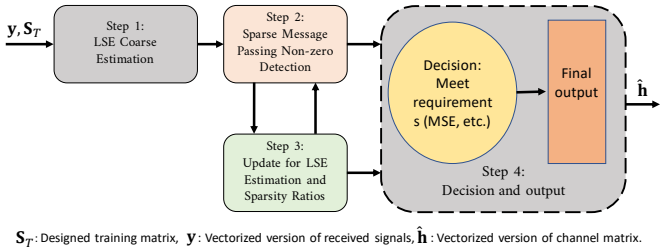


Figure 12. Block diagram of the message passing method proposed in [158].

low complexity recovery of the wideband beamspace channel is applied.

*Conclusions:* Table V provides a list of existing channel estimation techniques for systems with lens antenna arrays. Most of existing techniques employed the DFT lens array model, the single-carrier transmission and the TDD scheme, and assumed the channel reciprocity and a scenario of multiple single-antenna MTs. In this context, it will be useful to further study the channel estimation problem for wideband communications with different waveforms, also to further explore the path reciprocity assumption for existing works, and finally to consider the more general case of multi-antenna multi-user system. The message passing methods seem promising and worth more extensive research.

## VII. Channel Estimation Techniques for Systems with Few-Bit ADCs

It is well known that ADCs represent a high power consumption component of mmWave transceivers due to the large bandwidth [160], [161]. This is exacerbated for massive MIMO due to the large number of RF chains [162], where the power consumption of ADCs dominates the total power consumption of the whole RF chain [163]. Fortunately, the power consumption of ADCs is greatly reduced if the resolution is diminished to a few-bits - typically 1 to 4 bits -, hence the proposal for architectures with limited power consumption using low-resolution ADCs, known as *few-bit ADCs architectures*. An examination of lowering the ADCs's precision on the system performance was elaborated in [164], and several efforts ushered out the feasibility and benefit of these few-bit ADCs on the system performance compared to high-resolution power-hungry ADCs [162], [165]. Owing to the fact that few-bit ADCs are a strong candidate against high-resolution ADCs for mmWave systems, various works provided the capacity analysis of such tools on mmWave systems [67], [166]. In addition, [167]–[169] delivered some research studies concerning the hybrid mmWave architecture with few-bit ADCs, answering many inquiries about the number of RF chains and the number of ADC's bits required, in which an energy-rate trade-off exists.

The research activity on mmWave channel estimation algorithms for few-bit ADCs architectures is quite recent, and we believe that such efforts are significant enough to be highlighted in this section. In fact, the prime research works on channel estimation for few-bit ADCs focused on the single-user case, yet some works which dealt with the multi-user case were also carried out and illustrated in this section. A pionnering work of Mo et *al.* focuses on architectures with one-bit ADCs [127]. Sparsity of the channel was exploited to formulate the channel estimation problem as a 1-bit compressive sensing problem which had been already investigated in [170]. Thus, the proposed estimation algorithm - along with much of the proposed estimation algorithms that follow - was guided by the capitalized knowledge on quantized CS techniques [171]–[176] as well as on non-mmWave MIMO channel estimation algorithms for low-resolution receivers [177]–[179].

In the forthcoming subsections, we will explain how channel estimation with few-bit ADCs is applicable for both narrowband and wideband mmWave systems by presenting the research works that have been proposed for this objective. Following that, channel estimation with few-bit ADCs but for non-mmWave systems will be rapidly reviewed to convey the influence of low-resolution ADCs on channel estimation. In the end, we will present some other aspects of few-bit ADCs, such as capacity, performance under different beamforming schemes, and many more.

*Techniques for narrowband systems:* Although not realistic for the mmWave channel, the narrowband assumption can be considered as a starting point of research.

Traditionally, the channel estimation algorithms are based on a beamspace representation of the channel [75], [186] that takes advantage of the limited scattering of the mmWave environment and leads to a problem formulation that is adequate to compressive sensing techniques. In [127], some channel estimation algorithms are compared: The EM algorithm [177], [187], a modified version of EM that uses matching pursuit in lieu of maximum likelihood to exploit channel sparsity, and the generalized approximate message passing (GAMP) algorithm [39]. The latter was shown to have better performance in the low and medium SNR region. An adaptive one-bit CS scheme based on linear programming which does not require full optimization solving at each new measurement is proposed in [185]. New measurements are chosen adaptively with the aim of minimizing the region over which the final full optimization solving is done. However, the algorithm can not be extended to the case of few ($> 1$) bit ADCs. Furthermore, in this paper, oversampling is proposed to improve the channel estimation at low SNRs. The authors in [184] were the first to consider an adaptive CS solution adapted to the mmWave channel with few but $> 1$ bit ADCs. The problem is formulated as a sparse recovery problem from quantized and noisy measurements, and a modification of the generalized expectation maximization (GEM) algorithm [173], which is a CS algorithm for quantized and noisy measurements, was proposed and shown to provide equivalent or even better (at high SNRs and for average length training sequences) mean square error than the classical CS approach with a fixed dictionary. Figure 13 depicts the SU mmWave system in [184] with coarse quantization at the RX, where the feedback link is used to deliver the information about the selected training vectors to the TX where we have the codebook of the possible tranining vectors.

The authors in [183] and [182] presented an algorithm for estimating the AoAs and AoDs of the sparse channel.

This work is licensed under a Creative Commons Attribution 4.0 License. For more information, see https://creativecommons.org/licenses/by/4.0/.

This article has been accepted for publication in a future issue of this journal, but has not been fully edited. Content may change prior to final publication. Citation information: DOI 10.1109/OJCOMS.2020.3015394, IEEE Open Journal of the Communications Society



Table VI
CHANNEL ESTIMATION ALGORITHMS FOR MMWAVE SYSTEMS WITH FEW-BIT ADCS ARCHITECTURES.

| Reference | Year | Scenario | Some Assumptions | Architecture | UL/DL | 2D/3D | Complexity | Description |
|---|---|---|---|---|---|---|---|---|
| Kaushik *et al.* [125] | 2018 | Single-user | Narrowband | Hybrid | Not specified | 2D | $\mathcal{O}((N_T N_B)^2)$ | EM-SURE-GAMP |
| Sung *et al.* [126] | 2018 | Single-user | Narrowband | Hybrid | Not specified | 2D | Not specified | 1-bit GAMP, provided low estimation error |
| Mo *et al.* [69] | 2018 | Single-user | Wideband | Digital | Not specified | 3D | $\mathcal{O}(N_B N_T D \log(N_B N_T D))$ | AMP, showed that few-bit ADCs have a small amount of performance losses compared to infinite-precision ADCs |
| Wang *et al.* [180] | 2017 | Single-user or multi-user | Wideband | Digital | UL or DL | Not specified | $\mathcal{O}(K_s \log_2(K_s))$ | Performed similarly to an OFDM system with infinite-resolution ADCs |
| Rodriguez-fernandez *et al.* [181] | 2016 | Single-user | Narrowband | Hybrid | Not specified | 2D | Not specified | Modified EM, showed a satisfactory estimation error |
| Dong *et al.* [182] | 2016 | Single-user | Narrowband | Digital | UL | 2D | Not specified | Complex BIHT |
| Stockle *et al.* [183] | 2015 | Not specified | Narrowband | Digital | Not specified | 2D | $\mathcal{O}(NQn)$ | Complex BIHT |
| Rusu *et al.* [184] | 2015 | Single-user | Narrowband | Digital | Not specified | 2D | $\mathcal{O}(k \log(n/k))$ | AGEM, provided equivalent mean square error compared to CS approach |
| Rusu *et al.* [185] | 2015 | Single-user | Narrowband | Digital | Not specified | 2D | - | Adaptive 1-bit CS |
| Mo *et al.* [127] | 2014 | Single-user | Narrowband | Digital | Not specified | 3D | Not specified | Modified EM and GAMP, GAMP was shown to have better performance in the low and medium SNR region |

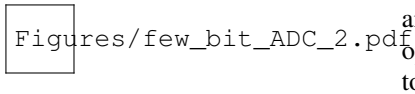


Figure 13. The SU mmWave system with coarse quantization at the receiver in [184]

Instead of using a basis pursuit denoise (BPDN) approach that considers the 1-bit measurements as signals corrupted by noise, they adapted to complex-valued measurements of the binary iterative hard thresholding (BIHT) algorithm described in [188] that takes explicitly the 1-bit nature of the measurement. The algorithm was shown to provide similar performance to BPDN while having lesser complexity. Another channel estimation algorithm for hybrid architecture in the SU scenario was proposed in [181]. The method is based on a modified version of the EM algorithm combined with MMSE estimation and OMP. The results of the proposed algorithm showed a satisfactory estimation error when using the low-resolution ADCs, and that using the high-resolution ADCs doesn't provide that much reduction of MSE. In [126] a channel estimation algorithm for low-resolution mmWave system was provided based on GAMP [189]. The proposed algorithm was compared to other variants of GAMP algorithms like the algorithm in [190] and the EM algorithm in [191], where it was shown that the proposed one-bit GAMP algorithm provides the lowest estimation error compared to these algorithms. Moreover, it was illustrated that the three GAMP-based algorithms perform better than the LSE without quantization. In [125], a mmWave channel estimation algorithm for low-resolution ADCs was proposed, in which the CS formulated estimation of the channel was solved with the aid of the Stein's unbiased risk estimate (SURE) [192] within the GAMP framework and by employing the EM [191]. The resulting EM-SURE-GAMP algorithm was compared to the EM-GAMP algorithm and was shown to exhibit better MSE performance than the latter in the low and high SNR regions.

*Techniques for wideband systems:* The work presented so far concentrated on the narrowband model, which is not a realistic assumption. However, over here we present the few works carried out for the wideband model. In [180] a channel estimation technique was proposed for SISO-OFDM mmWave system with low-resolution ADCs. The authors also developed an efficient data detection algorithm that achieves the Bayesian optimal design limits, and provided a power allocation scheme to reduce the symbol error rate. The results shown in the paper revealed that the proposed schemes perform similarly to an OFDM system with infinite-resolution ADCs. The work presented in [69] proposed a channel estimation algorithm with few-bit ADCs exploiting the sparsity of the channel in both the angle and delay domains. The estimation algorithm is based on the AMP algorithms. In particular, the authors proposed to use the GAMP algorithm detailed in [190] and the VAMP algorithms detailed in [193], [194], they also proposed a training sequence design and an FFT-based implementation that provides low complexity to the estimation process. The results of their paper [69] show that few-bit ADCs incur only small amount of performance losses compared to infinite-precision ADCs. It is worth noting that [69] is an extension of [127] in terms of ADCs precision and channel model, where a narrowband channel was assumed and one-bit ADCs were studied in [127]. Another work dealt with frequency selective channel estimation using 1-bit quantization for a multi-user uplink massive MIMO mmWave system was provided in [195]. A channel estimation algorithm was proposed based on the EM algorithm [177] combined with sparse recovery technique iterative hard thresholding (IHT) [106]. The proposed algorithm was shown to provide a good channel estimation performance through simulation results.

*Non-mmWave systems:* Under different conditions, some works dealt with the acquisition of channel information with the assumption of low-resolution ADCs but not for mmWave systems and channels. Some of these works include, [179] where a joint channel-and-data estimation algorithm for low-precision ADCs system was proposed based on the optimal Bayes estimator, and [196] where the bilinear generalized approximate message passing (BiG-AMP) technique was employed. A recent paper [197] studied channel estimation for multi-user uplink massive MIMO systems with 1-bit spatial sigma-delta ADCs. The authors explain the benefits of using the sigma-delta ADCs in reducing the noise on the signal, where it was shown through simulation results that the sigma-delta modulation reduces the quantization error of the low-resolution ADCs. The authors proposed to use the linear minimum mean squared estimator (LMMSE) to estimate the

This work is licensed under a Creative Commons Attribution 4.0 License. For more information, see https://creativecommons.org/licenses/by/4.0/.

This article has been accepted for publication in a future issue of this journal, but has not been fully edited. Content may change prior to final publication. Citation information: DOI 10.1109/OJCOMS.2020.3015394, IEEE Open Journal of the Communications Society



channel based on the Bussgang decomposition [198] which reformulates the non-linear quantizer model using an equivalent linear model plus quantization noise.

*Other aspects of few-bit ADCs systems:* Many papers studied the effects of low-resolution ADCs on mmWave systems for different aspects rather than channel estimation, including achievable throughput, achievable capacity, beamforming schemes and types, spectral and energy efficiency, codebook designs, and many more. One of these works is [199], where the authors studied the effects of low-resolution ADCs in two cases. First, they showed that the capacity of single-user SISO systems can be achieved by combining least-squares channel estimation with joint pilot and data symbols detection. Second, they showed that the use of maximum ratio combining jointly with least-squares channel estimation is adequate for the use of high-order constellation (example 16-QAM) in the case of multi-user uplink massive MIMO system. The authors in [200] provided a performance comparison between a system using hybrid beamforming and a system using digital beamforming, where the comparison was delivered for a multi-user scenario wideband mmWave system. Evaluations exhibited that for systems implementing low-resolution ADCs, the digital beamforming is more spectral and energy efficient than the hybrid one, and can convey a higher rate.

*Conclusions:* The high power cost of the RF chains in mmWave systems raises many questions mainly because a high power-hungry ADC is needed at each RF chain, this high power cost can be mitigated using few-bit ADCs. In this section we have presented the methods that have been proposed for mmWave channel estimation with few-bit ADCs. The popular ones are listed in Table VI. These works studied the narrowband and wideband systems. As we can see, all of them except [180] and [69] considered the narrowband case. Thus, more attention has to be appended for wideband case in the future. Thereafter, we have seen the importance of low-resolution ADCs for non-mmWave systems and some few other aspects of them.

## VIII. Discussion and Open Directions of Research

In this paper, we have provided a comprehensive overview of the state-of-the-art of channel estimation techniques for mmWave systems. A lot of work in this domain was conducted in the past few years as we have seen in the above sections. Existing techniques for hybrid architecture systems, for ones with lens antenna array and for ones with few-bit ADCs are respectively summarized in Tables II and IV, V and VI. However, a lot of work also remains to be done in order to develop efficient channel estimation techniques for mmWave cellular systems. We list in the following some identified future research directions.

- Duplexing techniques: At this stage the TDD is considered to be the best choice for mmWave systems. Recently, the FDD have gained more attention thanks to the huge available bandwidth in the mmWave frequency bands. Most of existing channel estimation methods assume that the employed duplexing technique is TDD. To the best of our knowledge, the only exception is the solution proposed in [86] for systems with lens antenna array. Thus it will be useful to come up with solutions that adapt to the FDD case for the three aforementioned system architectures.
- Wideband frequency-selective channels: The wide bandwidth available in the mmWave bands leads inevitably to frequency-selective channels since the different frequency components will experience independent fadings. This problem is traditionally solved by employing appropriate waveforms such as OFDM, filter bank multi-carrier (FBMC) or universal filtered multi-carrier (UFMC), among others, refer to [12] for more details. The channel estimation for wideband problem has been mainly studied for hybrid architecture with OFDM. This area must be further explored to cover all the architectures and all the waveforms in order to propose tailored channel estimation solutions and to try to keep up with the latest advances in this domain.
- Multi-user scenario: The application of mmWave communications to cellular systems implies to consider multi-user communications. This also requires to employ some multiple access scheme such as orthogonal frequency-division multiplexing access, semi-orthogonal multiple access scheme [201], or non-orthogonal multiple access [202]. Most of the above presented works either consider a single-user or several users with single-antenna per user, which is not realistic. The employed multiple access scheme must be taken into consideration in the design of channel estimation techniques. Furthermore, an additional effort must be dedicated to the pilot contamination problem which could limit the number of scheduled users and degrades the channel estimation accuracy.
- Graphical models: The channel estimation problem can be reformulated such as it can be represented in factor graph models which allows to employ the message passing algorithms as a powerful solution. This approach was exploited in the literature especially for the systems with few-bit ADCs where the GAMP is mainly used. It is promising to extend this effort to the other mmWave system architectures, and to other variations of message passing algorithms such as expectation-propagation algorithms and belief-propagation algorithms and their different approximations.
- Machine learning: It is not complicated to collect a large amount of wireless communications data which makes worth investigating if machine learning tools are capable to inspect the structure of the received signal and hence to estimate the mmWave channel. This idea becomes more legitimate with the recent advances in machine learning fields especially the deep learning which proposes several efficient tools such as deep convolutional neural networks, recurrent neural Networks, and Bayesian neural networks, and their different variations. For the time being, this axe of research was rarely studied, that is why it is deemed as promising and attractive.
- 3D : A 3D channel estimation means that neither the elevation scattering nor the horizontal scattering is neglected. Indeed, it is more practical to know the AoAs and

This work is licensed under a Creative Commons Attribution 4.0 License. For more information, see https://creativecommons.org/licenses/by/4.0/.

This article has been accepted for publication in a future issue of this journal, but has not been fully edited. Content may change prior to final publication. Citation information: DOI 10.1109/OJCOMS.2020.3015394, IEEE Open Journal of the Communications Society



the AoDs in both the horizontal and the vertical plans. A quick look on Tables II, IV, V and VI, shows that few papers studied the 3D channels estimation for mmWave systems with lens antennas arrays. Even in these papers, the 3D estimation was not combined with other assumptions like FDD, wideband channels, different waveforms, path reciprocity, multiple-antenna terminals. This issue must be fixed by introducing new 3D estimation solutions for the hybrid architectures and the ones with few-bit ADCs, and by including other realistic assumptions.

- Antenna array design: Beamforming gains are enabled by antenna arrays which are composed of several antenna elements that can be distributed via different geometrical configuration (linear, planar, circular) [203] and array layouts (uniform and non-uniform) [204]. All existing channels estimation works for hybrid architectures and the ones with few-bit ADCs assume a uniform linear planar geometry of the antenna array. It will be useful to adapt the channel estimation techniques according to the employed array configuration.
- High mobility : Accurate alignment of narrow beams of mmWave transmission is essential to avoid a significant loss in received power in the high mobility scenarios, such as vehicular mmWave systems, since the high mobility will increase the beam training and alignment overhead. In order to establish a stable link between the BS and the MT, the channel estimation, and hence the beam alignment, must be completed or joined with a beam tracking scheme in order to track the variations in AoDs/AoAs at the receiver. Despite the efforts deployed in this area [205], [206], some extensive research is needed to develop practical and fast estimation/tracking algorithms for mmWave channels.
- Quantization errors: In the literature, the beam steering directions are assumed to be quantized, i.e. the AoAs/AoDs are considered discrete against continuous ones in practice, which leads to quantization errors in channel estimation algorithms. The impact of this quantization errors on the performance of existing algorithms must be evaluated and new improved ones must be proposed if necessary.
- Cognitive radio: One solution to increase the spectral efficiency and to reply to the increasing traffic demand is to combine cognitive radio and mmWave communications, this perspective had been studied in several recent research works [207]–[209]. In this context, the problem of joint channel estimation and spectrum sensing for the secondary and the primary users must be further investigated.

## IX. Conclusions

This survey will serve as a useful review of the state-of-the-art of channel estimation techniques for mmWave massive MIMO communication systems. The systems design and the channel characteristics to be taken into consideration were first explained. Afterwards, we treated with a casual and non-analytical way the principal channel estimation methods so as to provide an essential knowledge on each one among them. This treatment was applied to the three main mmWave system architectures namely the hybrid architecture, the lens antenna array one, and the one with few-bit ADCs. However, the reader is recommended to further dig for more understanding of the details of each method.

## References


[1] Ericsson, "Ericsson Mobiliry Report," Stockholm, Sweden, Tech. Rep., Jun. 2019. [Online]. Available: https://www.ericsson.com/en/mobility-report/reports/june-2019

[2] M. Agiwal, A. Roy, and N. Saxena, "Next generation 5g wireless networks: A comprehensive survey," *IEEE Communications Surveys Tutorials*, vol. 18, no. 3, pp. 1617–1655, 2016.

[3] Y. Niu, Y. Li, D. Jin, L. Su, and A. V. Vasilakos, "A survey of millimeter wave communications (mmWave) for 5g: opportunities and challenges," *Wireless Networks*, vol. 21, no. 8, pp. 2657–2676, Nov. 2015.

[4] J. G. Andrews, T. Bai, M. N. Kulkarni, A. Alkhateeb, A. K. Gupta, and R. W. Heath, "Modeling and analyzing millimeter wave cellular systems," *IEEE Transactions on Communications*, vol. 65, no. 1, pp. 403–430, 2017.

[5] M. Xiao, S. Mumtaz, Y. Huang, L. Dai, Y. Li, M. Matthaiou, G. K. Karagiannidis, E. Bjrnson, K. Yang, C. I, and A. Ghosh, "Millimeter wave communications for future mobile networks," *IEEE Journal on Selected Areas in Communications*, vol. 35, no. 9, pp. 1909–1935, 2017.

[6] I. A. Hemadeh, K. Satyanarayana, M. El-Hajjar, and L. Hanzo, "Millimeter-wave communications: Physical channel models, design considerations, antenna constructions, and link-budget," *IEEE Communications Surveys Tutorials*, vol. 20, no. 2, pp. 870–913, 2018.

[7] T. S. Rappaport, Y. Xing, G. R. MacCartney, A. F. Molisch, E. Mellios, and J. Zhang, "Overview of millimeter wave communications for fifth-generation (5g) wireless networkswith a focus on propagation models," *IEEE Transactions on Antennas and Propagation*, vol. 65, no. 12, pp. 6213–6230, 2017.

[8] S. Mumtaz, J. Rodriguez, and L. Dai, *mmWave Massive MIMO - 1st Edition*. Elsevier, 2017.

[9] I. Ahmed, H. Khammari, A. Shahid, A. Musa, K. S. Kim, E. De Poorter, and I. Moerman, "A survey on hybrid beamforming techniques in 5g: Architecture and system model perspectives," *IEEE Communications Surveys Tutorials*, vol. 20, no. 4, pp. 3060–3097, 2018.

[10] X. Wang, L. Kong, F. Kong, F. Qiu, M. Xia, S. Arnon, and G. Chen, "Millimeter wave communication: A comprehensive survey," *IEEE Communications Surveys Tutorials*, vol. 20, no. 3, pp. 1616–1653, 2018.

[11] A. Naqvi and S. Lim, "Review of Recent Phased Arrays for Millimeter-Wave Wireless Communication," *Sensors*, vol. 18, no. 10, p. 3194, Sep. 2018.

[12] S. A. Busari, K. M. S. Huq, S. Mumtaz, L. Dai, and J. Rodriguez, "Millimeter-wave massive mimo communication for future wireless systems: A survey," *IEEE Communications Surveys Tutorials*, vol. 20, no. 2, pp. 836–869, 2018.

[13] L. Zhang, H. Zhao, S. Hou, Z. Zhao, H. Xu, X. Wu, Q. Wu, and R. Zhang, "A survey on 5g millimeter wave communications for uav-assisted wireless networks," *IEEE Access*, vol. 7, pp. 117 460–117 504, 2019.

[14] N. Al-Falahy and O. Y. Alani, "Millimetre wave frequency band as a candidate spectrum for 5g network architecture: A survey," *Physical Communication*, vol. 32, pp. 120–144, Feb. 2019.

[15] V. Va, T. Shimizu, G. Bansal, and R. W. Heath, *Millimeter Wave Vehicular Communications: A Survey*. Hanover, MA, USA: Now Publishers Inc., 2016.

[16] T. S. Rappaport, S. Sun, R. Mayzus, H. Zhao, Y. Azar, K. Wang, G. N. Wong, J. K. Schulz, M. Samimi, and F. Gutierrez, "Millimeter wave mobile communications for 5g cellular: It will work!" *IEEE Access*, vol. 1, pp. 335–349, 2013.

[17] W. Roh, J. Seol, J. Park, B. Lee, J. Lee, Y. Kim, J. Cho, K. Cheun, and F. Aryanfar, "Millimeter-wave beamforming as an enabling technology for 5g cellular communications: theoretical feasibility and prototype results," *IEEE Communications Magazine*, vol. 52, no. 2, pp. 106–113, 2014.

[18] A. Alkhateeb, J. Mo, N. Gonzalez-Prelcic, and R. W. Heath, "Mimo precoding and combining solutions for millimeter-wave systems," *IEEE Communications Magazine*, vol. 52, no. 12, pp. 122–131, 2014.


This work is licensed under a Creative Commons Attribution 4.0 License. For more information, see https://creativecommons.org/licenses/by/4.0/.

This article has been accepted for publication in a future issue of this journal, but has not been fully edited. Content may change prior to final publication. Citation information: DOI 10.1109/OJCOMS.2020.3015394, IEEE Open Journal of the Communications Society




[19] T. S. Rappaport, R. Heath, R. Daniels, and J. Murdock, *Millimeter Wave Wireless Communications*. Prentice Hall, 2015.

[20] "IEEE Standard for Information technology–Telecommunications and information exchange between systems–Local and metropolitan area networks–Specific requirements-Part 11: Wireless LAN Medium Access Control (MAC) and Physical Layer (PHY) Specifications Amendment 3: Enhancements for Very High Throughput in the 60 GHz Band," IEEE, Tech. Rep.

[21] "IEEE Standard for Information technology– Local and metropolitan area networks– Specific requirements– Part 15.3: Amendment 2: Millimeter-wave-based Alternative Physical Layer Extension," IEEE, Tech. Rep.

[22] WiGig, "Defining the Future of Multi-Gigabit Wireless Communications," White Paper, Jul. 2010.

[23] T. S. Rappaport, Y. Xing, O. Kanhere, S. Ju, A. Madanayake, S. Mandal, A. Alkhateeb, and G. C. Trichopoulos, "Wireless communications and applications above 100 ghz: Opportunities and challenges for 6g and beyond," *IEEE Access*, vol. 7, pp. 78 729–78 757, 2019.

[24] Samsung, "Feasibility of Mobility for 28 GHz millimeter-wave Systems," Tech. Rep., Sep. 2018.

[25] Huawei, "Deutsche Telekom and Huawei Complete World's First 5g High mmWave Technology over-the-air Field Tests," Feb. 2018. [Online]. Available: https://www.huawei.com/en/press-events/news/2018/2/DectschTelckom-5G-High-mmWave-Technology

[26] M. Marcus and B. Pattan, "Millimeter wave propagation: spectrum management implications," *IEEE Microwave Magazine*, vol. 6, no. 2, pp. 54–62, 2005.

[27] X. Zhang and J. G. Andrews, "Downlink cellular network analysis with multi-slope path loss models," *IEEE Transactions on Communications*, vol. 63, no. 5, pp. 1881–1894, 2015.

[28] S. Sun, G. R. MacCartney, and T. S. Rappaport, "Millimeter-wave distance-dependent large-scale propagation measurements and path loss models for outdoor and indoor 5g systems," in *2016 10th European Conference on Antennas and Propagation (EuCAP)*, 2016, pp. 1–5.

[29] M. R. Akdeniz, Y. Liu, M. K. Samimi, S. Sun, S. Rangan, T. S. Rappaport, and E. Erkip, "Millimeter wave channel modeling and cellular capacity evaluation," *IEEE Journal on Selected Areas in Communications*, vol. 32, no. 6, pp. 1164–1179, 2014.

[30] T. S. Rappaport, G. R. MacCartney, M. K. Samimi, and S. Sun, "Wideband millimeter-wave propagation measurements and channel models for future wireless communication system design," *IEEE Transactions on Communications*, vol. 63, no. 9, pp. 3029–3056, 2015.

[31] Y. Banday, G. Mohammad Rather, and G. R. Begh, "Effect of atmospheric absorption on millimetre wave frequencies for 5g cellular networks," *IET Communications*, vol. 13, no. 3, pp. 265–270, Feb. 2019.

[32] D. Nandi and A. Maitra, "Study of rain attenuation effects for 5g Mmwave cellular communication in tropical location," *IET Microwaves, Antennas & Propagation*, vol. 12, no. 9, pp. 1504–1507, Jul. 2018.

[33] H. Zhao, R. Mayzus, S. Sun, M. Samimi, J. K. Schulz, Y. Azar, K. Wang, G. N. Wong, F. Gutierrez, and T. S. Rappaport, "28 ghz millimeter wave cellular communication measurements for reflection and penetration loss in and around buildings in new york city," in *2013 IEEE International Conference on Communications (ICC)*, 2013, pp. 5163–5167.

[34] Z. Pi and F. Khan, "An introduction to millimeter-wave mobile broadband systems," *IEEE Communications Magazine*, vol. 49, no. 6, pp. 101–107, 2011.

[35] H. Technologies, "5g spectrum public policy position," Tech. Rep., 2017.

[36] FCC, "Use of Spectrum Bands Above 24 GHz for Mobile Radio Services," Tech. Rep. 84 FR 20810, 2019.

[37] Q. Xue, P. Zhou, X. Fang, and M. Xiao, "Performance analysis of interference and eavesdropping immunity in narrow beam mmwave networks," *IEEE Access*, vol. 6, pp. 67 611–67 624, 2018.

[38] E. Bjornson, L. Van der Perre, S. Buzzi, and E. G. Larsson, "Massive mimo in sub-6 ghz and mmwave: Physical, practical, and use-case differences," *IEEE Wireless Communications*, vol. 26, no. 2, pp. 100–108, 2019.

[39] S. Rangan, T. S. Rappaport, and E. Erkip, "Millimeter-wave cellular wireless networks: Potentials and challenges," *Proceedings of the IEEE*, vol. 102, no. 3, pp. 366–385, 2014.

[40] T. S. Rappaport, J. N. Murdock, and F. Gutierrez, "State of the art in 60-ghz integrated circuits and systems for wireless communications," *Proceedings of the IEEE*, vol. 99, no. 8, pp. 1390–1436, 2011.

[41] C. H. Doan, S. Emami, D. A. Sobel, A. M. Niknejad, and R. W. Brodersen, "Design considerations for 60 ghz cmos radios," *IEEE Communications Magazine*, vol. 42, no. 12, pp. 132–140, 2004.

[42] L. Zhao, "Millimeter Wave Systems for Wireless Cellular Communications," *arXiv:1811.12606 [cs, math]*, Nov. 2018, arXiv: 1811.12606.

[43] Shuguang Cui, A. J. Goldsmith, and A. Bahai, "Energy-efficiency of mimo and cooperative mimo techniques in sensor networks," *IEEE Journal on Selected Areas in Communications*, vol. 22, no. 6, pp. 1089–1098, 2004.

[44] Y. Teng, M. Liu, F. R. Yu, V. C. M. Leung, M. Song, and Y. Zhang, "Resource allocation for ultra-dense networks: A survey, some research issues and challenges," *IEEE Communications Surveys Tutorials*, vol. 21, no. 3, pp. 2134–2168, 2019.

[45] M. Kamel, W. Hamouda, and A. Youssef, "Ultra-dense networks: A survey," *IEEE Communications Surveys Tutorials*, vol. 18, no. 4, pp. 2522–2545, 2016.

[46] S. Han, C. I, Z. Xu, and C. Rowell, "Large-scale antenna systems with hybrid analog and digital beamforming for millimeter wave 5g," *IEEE Communications Magazine*, vol. 53, no. 1, pp. 186–194, 2015.

[47] M. Boers, B. Afshar, I. Vassiliou, S. Sarkar, S. T. Nicolson, E. Adabi, B. G. Perumana, T. Chalvatzis, S. Kavvadias, P. Sen, W. L. Chan, A. H. Yu, A. Parsa, M. Nariman, S. Yoon, A. G. Besoli, C. A. Kyriazidou, G. Zochios, J. A. Castaneda, T. Sowlati, M. Rofougaran, and A. Rofougaran, "A 16tx/16rx 60 ghz 802.11ad chipset with single coaxial interface and polarization diversity," *IEEE Journal of Solid-State Circuits*, vol. 49, no. 12, pp. 3031–3045, 2014.

[48] B. Biglarbegian, M. Fakharzadeh, D. Busuioc, M. Nezhad-Ahmadi, and S. Safavi-Naeini, "Optimized microstrip antenna arrays for emerging millimeter-wave wireless applications," *IEEE Transactions on Antennas and Propagation*, vol. 59, no. 5, pp. 1742–1747, 2011.

[49] S. Kutty and D. Sen, "Beamforming for millimeter wave communications: An inclusive survey," *IEEE Communications Surveys Tutorials*, vol. 18, no. 2, pp. 949–973, 2016.

[50] Junyi Wang, Zhou Lan, Chang-woo Pyo, T. Baykas, Chin-sean Sum, M. A. Rahman, Jing Gao, R. Funada, F. Kojima, H. Harada, and S. Kato, "Beam codebook based beamforming protocol for multi-gbps millimeter-wave wpan systems," *IEEE Journal on Selected Areas in Communications*, vol. 27, no. 8, pp. 1390–1399, 2009.

[51] S. Hur, T. Kim, D. J. Love, J. V. Krogmeier, T. A. Thomas, and A. Ghosh, "Multilevel millimeter wave beamforming for wireless backhaul," in *2011 IEEE GLOBECOM Workshops (GC Wkshps)*, 2011, pp. 253–257.

[52] ——, "Millimeter wave beamforming for wireless backhaul and access in small cell networks," *IEEE Transactions on Communications*, vol. 61, no. 10, pp. 4391–4403, 2013.

[53] P. Xia, S. Yong, J. Oh, and C. Ngo, "A practical sdma protocol for 60 ghz millimeter wave communications," in *2008 42nd Asilomar Conference on Signals, Systems and Computers*, 2008, pp. 2019–2023.

[54] P. Xia, H. Niu, J. Oh, and C. Ngo, "Practical antenna training for millimeter wave mimo communication," in *2008 IEEE 68th Vehicular Technology Conference*, 2008, pp. 1–5.

[55] P. Xia, S. Yong, J. Oh, and C. Ngo, "Multi-stage iterative antenna training for millimeter wave communications," in *IEEE GLOBECOM 2008 - 2008 IEEE Global Telecommunications Conference*, 2008, pp. 1–6.

[56] Z. Xiao, L. Bai, and J. Choi, "Iterative joint beamforming training with constant-amplitude phased arrays in millimeter-wave communications," *IEEE Communications Letters*, vol. 18, no. 5, pp. 829–832, 2014.

[57] Xinying Zhang, A. F. Molisch, and Sun-Yuan Kung, "Variable-phase-shift-based rf-baseband codesign for mimo antenna selection," *IEEE Transactions on Signal Processing*, vol. 53, no. 11, pp. 4091–4103, 2005.

[58] T. S. Rappaport, F. Gutierrez, E. Ben-Dor, J. N. Murdock, Y. Qiao, and J. I. Tamir, "Broadband millimeter-wave propagation measurements and models using adaptive-beam antennas for outdoor urban cellular communications," *IEEE Transactions on Antennas and Propagation*, vol. 61, no. 4, pp. 1850–1859, 2013.

[59] 3GPP, "Final report of {3GPP TSG RAN WG1} (85)," 3GPP, Tech. Rep., 2016.

[60] O. E. Ayach, S. Rajagopal, S. Abu-Surra, Z. Pi, and R. W. Heath, "Spatially sparse precoding in millimeter wave mimo systems," *IEEE Transactions on Wireless Communications*, vol. 13, no. 3, pp. 1499–1513, 2014.

[61] X. Gao, L. Dai, S. Han, C. I, and R. W. Heath, "Energy-efficient hybrid analog and digital precoding for mmwave mimo systems with large antenna arrays," *IEEE Journal on Selected Areas in Communications*, vol. 34, no. 4, pp. 998–1009, 2016.


This work is licensed under a Creative Commons Attribution 4.0 License. For more information, see https://creativecommons.org/licenses/by/4.0/.

This article has been accepted for publication in a future issue of this journal, but has not been fully edited. Content may change prior to final publication. Citation information: DOI 10.1109/OJCOMS.2020.3015394, IEEE Open Journal of the Communications Society




[62] R. Mndez-Rial, C. Rusu, N. Gonzlez-Prelcic, A. Alkhateeb, and R. W. Heath, "Hybrid mimo architectures for millimeter wave communications: Phase shifters or switches?" *IEEE Access*, vol. 4, pp. 247–267, 2016.

[63] A. Alkhateeb, Y. Nam, J. Zhang, and R. W. Heath, "Massive mimo combining with switches," *IEEE Wireless Communications Letters*, vol. 5, no. 3, pp. 232–235, 2016.

[64] S. Payami, N. Mysore Balasubramanya, C. Masouros, and M. Sellathurai, "Phase shifters versus switches: An energy efficiency perspective on hybrid beamforming," *IEEE Wireless Communications Letters*, vol. 8, no. 1, pp. 13–16, 2019.

[65] J. Brady, N. Behdad, and A. M. Sayeed, "Beamspace mimo for millimeter-wave communications: System architecture, modeling, analysis, and measurements," *IEEE Transactions on Antennas and Propagation*, vol. 61, no. 7, pp. 3814–3827, 2013.

[66] Y. Zeng and R. Zhang, "Millimeter wave mimo with lens antenna array: A new path division multiplexing paradigm," *IEEE Transactions on Communications*, vol. 64, no. 4, pp. 1557–1571, 2016.

[67] J. Mo and R. W. Heath, "Capacity analysis of one-bit quantized mimo systems with transmitter channel state information," *IEEE Transactions on Signal Processing*, vol. 63, no. 20, pp. 5498–5512, 2015.

[68] T. Zhang, C. Wen, S. Jin, and T. Jiang, "Mixed-adc massive mimo detectors: Performance analysis and design optimization," *IEEE Transactions on Wireless Communications*, vol. 15, no. 11, pp. 7738–7752, 2016.

[69] J. Mo, P. Schniter, and R. W. Heath, "Channel estimation in broadband millimeter wave mimo systems with few-bit adcs," *IEEE Transactions on Signal Processing*, vol. 66, no. 5, pp. 1141–1154, 2018.

[70] H. He, C. Wen, and S. Jin, "Bayesian optimal data detector for hybrid mmwave mimo-ofdm systems with low-resolution adcs," *IEEE Journal of Selected Topics in Signal Processing*, vol. 12, no. 3, pp. 469–483, 2018.

[71] A. Alkhateeb, O. El Ayach, G. Leus, and R. W. Heath, "Channel estimation and hybrid precoding for millimeter wave cellular systems," *IEEE Journal of Selected Topics in Signal Processing*, vol. 8, no. 5, pp. 831–846, 2014.

[72] M. N. Kulkarni, A. Ghosh, and J. G. Andrews, "A comparison of mimo techniques in downlink millimeter wave cellular networks with hybrid beamforming," *IEEE Transactions on Communications*, vol. 64, no. 5, pp. 1952–1967, 2016.

[73] A. M. Sayeed, "A virtual mimo channel representation and applications," in *IEEE Military Communications Conference, 2003. MILCOM 2003.*, vol. 1, 2003, pp. 615–620 Vol.1.

[74] J. P. Gonzlez-Coma, J. Rodrguez-Fernndez, N. Gonzlez-Prelcic, L. Castedo, and R. W. Heath, "Channel estimation and hybrid precoding for frequency selective multiuser mmwave mimo systems," *IEEE Journal of Selected Topics in Signal Processing*, vol. 12, no. 2, pp. 353–367, 2018.

[75] R. W. Heath, N. Gonzlez-Prelcic, S. Rangan, W. Roh, and A. M. Sayeed, "An overview of signal processing techniques for millimeter wave mimo systems," *IEEE Journal of Selected Topics in Signal Processing*, vol. 10, no. 3, pp. 436–453, 2016.

[76] W. Tan, S. D. Assimonis, M. Matthaiou, Y. Han, X. Li, and S. Jin, "Analysis of different planar antenna arrays for mmwave massive mimo systems," in *2017 IEEE 85th Vehicular Technology Conference (VTC Spring)*, 2017, pp. 1–5.

[77] A. Kammoun, H. Khanfir, Z. Altman, M. Debbah, and M. Kamoun, "Preliminary results on 3d channel modeling: From theory to standardization," *IEEE Journal on Selected Areas in Communications*, vol. 32, no. 6, pp. 1219–1229, 2014.

[78] M. Dong, W. Chan, T. Kim, K. Liu, H. Huang, and G. Wang, "Simulation study on millimeter wave 3d beamforming systems in urban outdoor multi-cell scenarios using 3d ray tracing," in *2015 IEEE 26th Annual International Symposium on Personal, Indoor, and Mobile Radio Communications (PIMRC)*, 2015, pp. 2265–2270.

[79] D.-W. Yue, S. Xu, and H. H. Nguyen, "Diversity gain of millimeter-wave massive MIMO systems with distributed antenna arrays," *EURASIP Journal on Wireless Communications and Networking*, vol. 2019, no. 1, p. 54, Mar. 2019.

[80] R. Shafin, L. Liu, J. Zhang, and Y. Wu, "Doa estimation and capacity analysis for 3-d millimeter wave massive-mimo/fd-mimo ofdm systems," *IEEE Transactions on Wireless Communications*, vol. 15, no. 10, pp. 6963–6978, 2016.

[81] W. Ma and C. Qi, "Channel estimation for 3-d lens millimeter wave massive mimo system," *IEEE Communications Letters*, vol. 21, no. 9, pp. 2045–2048, 2017.

[82] T. Cheng, Y. Song, T. Li, F. Li, and H. Liu, "Low-complexity channel estimation in 3d lens millimeter-wave massive mimo systems," in *2018 24th Asia-Pacific Conference on Communications (APCC)*, 2018, pp. 347–352.

[83] X. Gao, L. Dai, S. Han, C. I, and X. Wang, "Reliable beamspace channel estimation for millimeter-wave massive mimo systems with lens antenna array," *IEEE Transactions on Wireless Communications*, vol. 16, no. 9, pp. 6010–6021, 2017.

[84] X. Gao, L. Dai, S. Zhou, A. M. Sayeed, and L. Hanzo, "Beamspace channel estimation for wideband millimeter-wave mimo with lens antenna array," in *2018 IEEE International Conference on Communications (ICC)*, 2018, pp. 1–6.

[85] Y. Zeng, L. Yang, and R. Zhang, "Multi-user millimeter wave mimo with full-dimensional lens antenna array," *IEEE Transactions on Wireless Communications*, vol. 17, no. 4, pp. 2800–2814, 2018.

[86] L. Yang, Y. Zeng, and R. Zhang, "Channel estimation for millimeter-wave mimo communications with lens antenna arrays," *IEEE Transactions on Vehicular Technology*, vol. 67, no. 4, pp. 3239–3251, 2018.

[87] A. F. Molisch, *Wireless Communications*, 2nd ed. Wiley-IEEE Press, 2011.

[88] P. Schniter and A. Sayeed, "Channel estimation and precoder design for millimeter-wave communications: The sparse way," in *2014 48th Asilomar Conference on Signals, Systems and Computers*, 2014, pp. 273–277.

[89] A. Ghosh, T. A. Thomas, M. C. Cudak, R. Ratasuk, P. Moorut, F. W. Vook, T. S. Rappaport, G. R. MacCartney, S. Sun, and S. Nie, "Millimeter-wave enhanced local area systems: A high-data-rate approach for future wireless networks," *IEEE Journal on Selected Areas in Communications*, vol. 32, no. 6, pp. 1152–1163, 2014.

[90] S. Sun and T. S. Rappaport, "Millimeter wave mimo channel estimation based on adaptive compressed sensing," in *2017 IEEE International Conference on Communications Workshops (ICC Workshops)*, 2017, pp. 47–53.

[91] E. J. Cands and M. B. Wakin, "An Introduction To Compressive Sampling [A sensing/sampling paradigm that goes against the common knowledge in data acquisition]," *IEEE Signal Processing Magazine*, vol. 25, pp. 21–30, Mar. 2008.

[92] R. G. Baraniuk, "Compressive sensing [lecture notes]," *IEEE Signal Processing Magazine*, vol. 24, no. 4, pp. 118–121, 2007.

[93] D. L. Donoho, A. Maleki, and A. Montanari, "Message-passing algorithms for compressed sensing," *Proceedings of the National Academy of Sciences*, vol. 106, no. 45, pp. 18 914–18 919, Nov. 2009.

[94] J. W. Choi, B. Shim, Y. Ding, B. Rao, and D. I. Kim, "Compressed sensing for wireless communications: Useful tips and tricks," *IEEE Communications Surveys Tutorials*, vol. 19, no. 3, pp. 1527–1550, 2017.

[95] E. J. Candes, J. Romberg, and T. Tao, "Robust uncertainty principles: exact signal reconstruction from highly incomplete frequency information," *IEEE Transactions on Information Theory*, vol. 52, no. 2, pp. 489–509, 2006.

[96] D. L. Donoho and M. Elad, "Optimally sparse representation in general (nonorthogonal) dictionaries via 1 minimization," *Proceedings of the National Academy of Sciences*, vol. 100, no. 5, pp. 2197–2202, Mar. 2003.

[97] E. J. Candes and T. Tao, "Decoding by linear programming," *IEEE Transactions on Information Theory*, vol. 51, no. 12, pp. 4203–4215, 2005.

[98] J. A. Tropp and A. C. Gilbert, "Signal recovery from random measurements via orthogonal matching pursuit," *IEEE Transactions on Information Theory*, vol. 53, no. 12, pp. 4655–4666, 2007.

[99] M. Rani, S. B. Dhok, and R. B. Deshmukh, "A systematic review of compressive sensing: Concepts, implementations and applications," *IEEE Access*, vol. 6, pp. 4875–4894, 2018.

[100] S. Chen, D. Donoho, and M. Saunders, "Atomic Decomposition by Basis Pursuit," *SIAM Review*, vol. 43, no. 1, pp. 129–159, Jan. 2001.

[101] E. Candes and T. Tao, "The Dantzig selector: Statistical estimation when p is much larger than n," *The Annals of Statistics*, vol. 35, no. 6, pp. 2313–2351, Dec. 2007.

[102] "Regression Shrinkage and Selection Via the Lasso - Tibshirani - 1996 - Journal of the Royal Statistical Society: Series B (Methodological) - Wiley Online Library." [Online]. Available: https://rss.onlinelibrary.wiley.com/doi/abs/10.1111/j.2517-6161.1996.tb02080.x

[103] S. G. Mallat and Zhifeng Zhang, "Matching pursuits with time-frequency dictionaries," *IEEE Transactions on Signal Processing*, vol. 41, no. 12, pp. 3397–3415, 1993.


This work is licensed under a Creative Commons Attribution 4.0 License. For more information, see https://creativecommons.org/licenses/by/4.0/.

This article has been accepted for publication in a future issue of this journal, but has not been fully edited. Content may change prior to final publication. Citation information: DOI 10.1109/OJCOMS.2020.3015394, IEEE Open Journal of the Communications Society




[104] J. Lee, G. Gil, and Y. H. Lee, "Exploiting spatial sparsity for estimating channels of hybrid mimo systems in millimeter wave communications," in *2014 IEEE Global Communications Conference*, 2014, pp. 3326–3331.

[105] D. Needell and J. Tropp, "CoSaMP: Iterative signal recovery from incomplete and inaccurate samples," *Applied and Computational Harmonic Analysis*, vol. 26, no. 3, pp. 301–321, May 2009.

[106] T. Blumensath and M. E. Davies, "Iterative hard thresholding for compressed sensing," *Applied and Computational Harmonic Analysis*, vol. 27, no. 3, pp. 265–274, Nov. 2009.

[107] S. Ji, Y. Xue, and L. Carin, "Bayesian compressive sensing," *IEEE Transactions on Signal Processing*, vol. 56, no. 6, pp. 2346–2356, 2008.

[108] J. A. Tropp and A. C. Gilbert, "Signal recovery from partial information via Orthogonal Matching Pursuit," *Ieee Trans. Inform. Theory*, 2005.

[109] J. Haupt and R. Nowak, "Signal reconstruction from noisy random projections," *IEEE Transactions on Information Theory*, vol. 52, no. 9, pp. 4036–4048, 2006.

[110] S. Kwon, J. Wang, and B. Shim, "Multipath matching pursuit," *IEEE Transactions on Information Theory*, vol. 60, no. 5, pp. 2986–3001, 2014.

[111] J. Wang, S. Kwon, and B. Shim, "Generalized orthogonal matching pursuit," *IEEE Transactions on Signal Processing*, vol. 60, no. 12, pp. 6202–6216, 2012.

[112] A. N. Uwaechia and N. M. Mahyuddin, "Stage-determined matching pursuit for sparse channel estimation in ofdm systems," *IEEE Systems Journal*, vol. 13, no. 3, pp. 2240–2251, 2019.

[113] A. Alkhateeb, O. El Ayach, G. Leus, and R. W. Heath, "Single-sided adaptive estimation of multi-path millimeter wave channels," in *2014 IEEE 15th International Workshop on Signal Processing Advances in Wireless Communications (SPAWC)*, 2014, pp. 125–129.

[114] Y. Peng, Y. Li, and P. Wang, "An enhanced channel estimation method for millimeter wave systems with massive antenna arrays," *IEEE Communications Letters*, vol. 19, no. 9, pp. 1592–1595, 2015.

[115] R. Mndez-Rial, C. Rusu, A. Alkhateeb, N. Gonzlez-Prelcic, and R. W. Heath, "Channel estimation and hybrid combining for mmwave: Phase shifters or switches?" in *2015 Information Theory and Applications Workshop (ITA)*, 2015, pp. 90–97.

[116] H. Chiang, T. Kadur, W. Rave, and G. Fettweis, "Low-complexity spatial channel estimation and hybrid beamforming for millimeter wave links," in *2016 IEEE 27th Annual International Symposium on Personal, Indoor, and Mobile Radio Communications (PIMRC)*, 2016, pp. 1–7.

[117] Y. Han and J. Lee, "Asymmetric channel estimation for multi-user millimeter wave communications," in *2016 International Conference on Information and Communication Technology Convergence (ICTC)*, 2016, pp. 4–6.

[118] S. Park and R. W. Heath, "Spatial channel covariance estimation for mmwave hybrid mimo architecture," in *2016 50th Asilomar Conference on Signals, Systems and Computers*, 2016, pp. 1424–1428.

[119] K. Venugopal, A. Alkhateeb, R. W. Heath, and N. G. Prelcic, "Time-domain channel estimation for wideband millimeter wave systems with hybrid architecture," in *2017 IEEE International Conference on Acoustics, Speech and Signal Processing (ICASSP)*, 2017, pp. 6493–6497.

[120] K. Venugopal, A. Alkhateeb, N. Gonzlez Prelcic, and R. W. Heath, "Channel estimation for hybrid architecture-based wideband millimeter wave systems," *IEEE Journal on Selected Areas in Communications*, vol. 35, no. 9, pp. 1996–2009, 2017.

[121] J. Rodrguez-Fernndez, K. Venugopal, N. Gonzlez-Prelcic, and R. W. Heath, "A frequency-domain approach to wideband channel estimation in millimeter wave systems," in *2017 IEEE International Conference on Communications (ICC)*, 2017, pp. 1–7.

[122] J. Rodrguez-Fernndez, N. Gonzlez-Prelcic, K. Venugopal, and R. W. Heath, "Frequency-domain compressive channel estimation for frequency-selective hybrid millimeter wave mimo systems," *IEEE Transactions on Wireless Communications*, vol. 17, no. 5, pp. 2946–2960, 2018.

[123] Z. Gao, C. Hu, L. Dai, and Z. Wang, "Channel estimation for millimeter-wave massive mimo with hybrid precoding over frequency-selective fading channels," *IEEE Communications Letters*, vol. 20, no. 6, pp. 1259–1262, 2016.

[124] D. C. Arajo, A. L. F. de Almeida, J. Axns, and J. C. M. Mota, "Channel estimation for millimeter-wave very-large mimo systems," in *2014 22nd European Signal Processing Conference (EUSIPCO)*, 2014, pp. 81–85.

[125] A. Kaushik, E. Vlachos, J. Thompson, and A. Perelli, "Efficient channel estimation in millimeter wave hybrid mimo systems with low resolution adcs," in *2018 26th European Signal Processing Conference (EUSIPCO)*, 2018, pp. 1825–1829.

[126] J. Sung, J. Choi, and B. L. Evans, "Narrowband channel estimation for hybrid beamforming millimeter wave communication systems with one-bit quantization," in *2018 IEEE International Conference on Acoustics, Speech and Signal Processing (ICASSP)*, 2018, pp. 3914–3918.

[127] J. Mo, P. Schniter, N. G. Prelcic, and R. W. Heath, "Channel estimation in millimeter wave mimo systems with one-bit quantization," in *2014 48th Asilomar Conference on Signals, Systems and Computers*, 2014, pp. 957–961.

[128] M. L. Malloy and R. D. Nowak, "Near-optimal adaptive compressed sensing," *IEEE Transactions on Information Theory*, vol. 60, no. 7, pp. 4001–4012, 2014.

[129] M. L. Malloy and R. D. Nowak, "Near-Optimal Compressive Binary Search," *arXiv:1203.1804 [cs, math]*, Mar. 2012, arXiv: 1203.1804.

[130] D. E. Berraki, S. M. D. Armour, and A. R. Nix, "Application of compressive sensing in sparse spatial channel recovery for beamforming in mmwave outdoor systems," in *2014 IEEE Wireless Communications and Networking Conference (WCNC)*, 2014, pp. 887–892.

[131] Z. Marzi, D. Ramasamy, and U. Madhow, "Compressive channel estimation and tracking for large arrays in mm-wave picocells," *IEEE Journal of Selected Topics in Signal Processing*, vol. 10, no. 3, pp. 514–527, 2016.

[132] Z. Xiao, P. Xia, and X. Xia, "Channel estimation and hybrid precoding for millimeter-wave mimo systems: A low-complexity overall solution," *IEEE Access*, vol. 5, pp. 16 100–16 110, 2017.

[133] J. He, T. Kim, H. Ghauch, K. Liu, and G. Wang, "Millimeter wave mimo channel tracking systems," in *2014 IEEE Globecom Workshops (GC Wkshps)*, 2014, pp. 416–421.

[134] S. Payami, M. Shariat, M. Ghoraishi, and M. Dianati, "Effective rf codebook design and channel estimation for millimeter wave communication systems," in *2015 IEEE International Conference on Communication Workshop (ICCW)*, 2015, pp. 1226–1231.

[135] M. Kokshoorn, P. Wang, Y. Li, and B. Vucetic, "Fast channel estimation for millimetre wave wireless systems using overlapped beam patterns," in *2015 IEEE International Conference on Communications (ICC)*, 2015, pp. 1304–1309.

[136] S. Montagner, N. Benvenuto, and P. Baracca, "Channel estimation using a 2d dft for millimeter-wave systems," in *2015 IEEE 81st Vehicular Technology Conference (VTC Spring)*, 2015, pp. 1–5.

[137] L. Wenl, Z. Weixia, and L. Xuefeng, "An adaptive channel estimation algorithm for millimeter wave cellular systems," *Journal of Communications and Information Networks*, vol. 1, no. 2, pp. 37–44, 2016.

[138] Z. Zhou, J. Fang, L. Yang, H. Li, Z. Chen, and S. Li, "Channel estimation for millimeter-wave multiuser mimo systems via parafac decomposition," *IEEE Transactions on Wireless Communications*, vol. 15, no. 11, pp. 7501–7516, 2016.

[139] Z. Guo, X. Wang, and W. Heng, "Millimeter-wave channel estimation based on 2-d beamspace music method," *IEEE Transactions on Wireless Communications*, vol. 16, no. 8, pp. 5384–5394, 2017.

[140] Y. Xiao, Y. Wang, and W. Xiang, "Dimension-deficient channel estimation of hybrid beamforming based on compressive sensing," *IEEE Access*, vol. 7, pp. 13 791–13 798, 2019.

[141] W. U. Bajwa, A. Sayeed, and R. Nowak, "Compressed sensing of wireless channels in time, frequency, and space," in *2008 42nd Asilomar Conference on Signals, Systems and Computers*, 2008, pp. 2048–2052.

[142] S. F. Cotter, B. D. Rao, Kjersti Engan, and K. Kreutz-Delgado, "Sparse solutions to linear inverse problems with multiple measurement vectors," *IEEE Transactions on Signal Processing*, vol. 53, no. 7, pp. 2477–2488, 2005.

[143] A. Cichocki, D. Mandic, L. De Lathauwer, G. Zhou, Q. Zhao, C. Caiafa, and H. A. PHAN, "Tensor decompositions for signal processing applications: From two-way to multiway component analysis," *IEEE Signal Processing Magazine*, vol. 32, no. 2, pp. 145–163, 2015.

[144] Z. Zhou, J. Fang, L. Yang, H. Li, Z. Chen, and R. S. Blum, "Low-rank tensor decomposition-aided channel estimation for millimeter wave mimo-ofdm systems," *IEEE Journal on Selected Areas in Communications*, vol. 35, no. 7, pp. 1524–1538, 2017.

[145] J. A. Tropp, A. C. Gilbert, and M. J. Strauss, "Simultaneous sparse approximation via greedy pursuit," in *Proceedings. (ICASSP '05). IEEE International Conference on Acoustics, Speech, and Signal Processing, 2005.*, vol. 5, 2005, pp. v/721–v/724 Vol. 5.

[146] Z. Gao, L. Dai, and Z. Wang, "Channel estimation for mmwave massive mimo based access and backhaul in ultra-dense network," in *2016 IEEE International Conference on Communications (ICC)*, 2016, pp. 1–6.


This work is licensed under a Creative Commons Attribution 4.0 License. For more information, see https://creativecommons.org/licenses/by/4.0/.

This article has been accepted for publication in a future issue of this journal, but has not been fully edited. Content may change prior to final publication. Citation information: DOI 10.1109/OJCOMS.2020.3015394, IEEE Open Journal of the Communications Society




[147] L. Dai, X. Gao, S. Han, I. Chih-Lin, and X. Wang, "Beamspace channel estimation for millimeter-wave massive mimo systems with lens antenna array," in *2016 IEEE/CIC International Conference on Communications in China (ICCC)*, 2016, pp. 1–6.

[148] L. Yang, Y. Zeng, and R. Zhang, "Efficient channel estimation for millimeter wave mimo with limited rf chains," in *2016 IEEE International Conference on Communications (ICC)*, 2016, pp. 1–6.

[149] J. Hogan and A. Sayeed, "Beam selection for performance-complexity optimization in high-dimensional mimo systems," in *2016 Annual Conference on Information Science and Systems (CISS)*, 2016, pp. 337–342.

[150] P. V. Amadori and C. Masouros, "Low rf-complexity millimeter-wave beamspace-mimo systems by beam selection," *IEEE Transactions on Communications*, vol. 63, no. 6, pp. 2212–2223, 2015.

[151] X. Gao, L. Dai, S. Han, I. Chih-Lin, and F. Adachi, "Beamspace channel estimation for 3d lens-based millimeter-wave massive mimo systems," in *2016 8th International Conference on Wireless Communications Signal Processing (WCSP)*, 2016, pp. 1–5.

[152] A. Sayeed and J. Brady, "Beamspace mimo for high-dimensional multiuser communication at millimeter-wave frequencies," in *2013 IEEE Global Communications Conference (GLOBECOM)*, 2013, pp. 3679–3684.

[153] G. H. Song, J. Brady, and A. Sayeed, "Beamspace mimo transceivers for low-complexity and near-optimal communication at mm-wave frequencies," in *2013 IEEE International Conference on Acoustics, Speech and Signal Processing*, 2013, pp. 4394–4398.

[154] M. Sadek, A. Tarighat, and A. H. Sayed, "Active antenna selection in multiuser mimo communications," *IEEE Transactions on Signal Processing*, vol. 55, no. 4, pp. 1498–1510, 2007.

[155] I. Berenguer, Xiaodong Wang, and V. Krishnamurthy, "Adaptive mimo antenna selection via discrete stochastic optimization," *IEEE Transactions on Signal Processing*, vol. 53, no. 11, pp. 4315–4329, 2005.

[156] S. L. H. Nguyen and A. Ghrayeb, "Compressive sensing-based channel estimation for massive multiuser mimo systems," in *2013 IEEE Wireless Communications and Networking Conference (WCNC)*, 2013, pp. 2890–2895.

[157] Z. Wan, Z. Gao, B. Shim, K. Yang, G. Mao, and M. Alouini, "Compressive sensing based channel estimation for millimeter-wave full-dimensional mimo with lens-array," *IEEE Transactions on Vehicular Technology*, vol. 69, no. 2, pp. 2337–2342, 2020.

[158] C. Huang, L. Liu, C. Yuen, and S. Sun, "Iterative channel estimation using lse and sparse message passing for mmwave mimo systems," *IEEE Transactions on Signal Processing*, vol. 67, no. 1, pp. 245–259, 2019.

[159] H. He, C. Wen, S. Jin, and G. Y. Li, "Deep learning-based channel estimation for beamspace mmwave massive mimo systems," *IEEE Wireless Communications Letters*, vol. 7, no. 5, pp. 852–855, 2018.

[160] R. H. Walden, "Analog-to-digital converter survey and analysis," *IEEE Journal on Selected Areas in Communications*, vol. 17, no. 4, pp. 539–550, 1999.

[161] S. Rapuano, P. Daponte, E. Balestrieri, L. De Vito, S. J. Tilden, S. Max, and J. Blair, "Adc parameters and characteristics," *IEEE Instrumentation Measurement Magazine*, vol. 8, no. 5, pp. 44–54, 2005.

[162] N. Liang and W. Zhang, "Mixed-adc massive mimo," *IEEE Journal on Selected Areas in Communications*, vol. 34, no. 4, pp. 983–997, 2016.

[163] J. Zhang, L. Dai, X. Li, Y. Liu, and L. Hanzo, "On low-resolution adcs in practical 5g millimeter-wave massive mimo systems," *IEEE Communications Magazine*, vol. 56, no. 7, pp. 205–211, 2018.

[164] J. Singh, O. Dabeer, and U. Madhow, "On the limits of communication with low-precision analog-to-digital conversion at the receiver," *IEEE Transactions on Communications*, vol. 57, no. 12, pp. 3629–3639, 2009.

[165] O. Orhan, E. Erkip, and S. Rangan, "Low power analog-to-digital conversion in millimeter wave systems: Impact of resolution and bandwidth on performance," in *2015 Information Theory and Applications Workshop (ITA)*, 2015, pp. 191–198.

[166] J. Mo and R. W. Heath, "High snr capacity of millimeter wave mimo systems with one-bit quantization," in *2014 Information Theory and Applications Workshop (ITA)*, 2014, pp. 1–5.

[167] W. B. Abbas, F. Gomez-Cuba, and M. Zorzi, "Millimeter wave receiver efficiency: A comprehensive comparison of beamforming schemes with low resolution adcs," *IEEE Transactions on Wireless Communications*, vol. 16, no. 12, pp. 8131–8146, 2017.

[168] J. Mo, A. Alkhateeb, S. Abu-Surra, and R. W. Heath, "Hybrid architectures with few-bit adc receivers: Achievable rates and energy-rate tradeoffs," *IEEE Transactions on Wireless Communications*, vol. 16, no. 4, pp. 2274–2287, 2017.

[169] J. Choi, B. L. Evans, and A. Gatherer, "Resolution-adaptive hybrid mimo architectures for millimeter wave communications," *IEEE Transactions on Signal Processing*, vol. 65, no. 23, pp. 6201–6216, 2017.

[170] P. T. Boufounos and R. G. Baraniuk, "1-bit compressive sensing," in *2008 42nd Annual Conference on Information Sciences and Systems*, 2008, pp. 16–21.

[171] T. Blumensath and M. E. Davies, "Normalized iterative hard thresholding: Guaranteed stability and performance," *IEEE Journal of Selected Topics in Signal Processing*, vol. 4, no. 2, pp. 298–309, 2010.

[172] A. Zymnis, S. Boyd, and E. Candes, "Compressed sensing with quantized measurements," *IEEE Signal Processing Letters*, vol. 17, no. 2, pp. 149–152, 2010.

[173] K. Qiu and A. Dogandzic, "Sparse signal reconstruction from quantized noisy measurements via gem hard thresholding," *IEEE Transactions on Signal Processing*, vol. 60, no. 5, pp. 2628–2634, 2012.

[174] Y. Plan and R. Vershynin, "Robust 1-bit compressed sensing and sparse logistic regression: A convex programming approach," *IEEE Transactions on Information Theory*, vol. 59, no. 1, pp. 482–494, 2013.

[175] L. Zhang, J. Yi, and R. Jin, "Efficient Algorithms for Robust One-bit Compressive Sensing," in *International Conference on Machine Learning*, Jan. 2014, pp. 820–828.

[176] K. Knudson, R. Saab, and R. Ward, "One-bit compressive sensing with norm estimation," *IEEE Transactions on Information Theory*, vol. 62, no. 5, pp. 2748–2758, 2016.

[177] A. Mezghani, F. Antreich, and J. A. Nossek, "Multiple parameter estimation with quantized channel output," in *2010 International ITG Workshop on Smart Antennas (WSA)*, 2010, pp. 143–150.

[178] O. Dabeer and U. Madhow, "Channel estimation with low-precision analog-to-digital conversion," in *2010 IEEE International Conference on Communications*, 2010, pp. 1–6.

[179] C. Wen, C. Wang, S. Jin, K. Wong, and P. Ting, "Bayes-optimal joint channel-and-data estimation for massive mimo with low-precision adcs," *IEEE Transactions on Signal Processing*, vol. 64, no. 10, pp. 2541–2556, 2016.

[180] H. Wang, C. Wen, and S. Jin, "Bayesian optimal data detector for mmwave ofdm system with low-resolution adc," *IEEE Journal on Selected Areas in Communications*, vol. 35, no. 9, pp. 1962–1979, 2017.

[181] J. Rodrguez-Fernndez, N. Gonzlez-Prelcic, and R. W. Heath, "Channel estimation in mixed hybrid-low resolution mimo architectures for mmwave communication," in *2016 50th Asilomar Conference on Signals, Systems and Computers*, 2016, pp. 768–773.

[182] Y. Dong, C. Chen, and Y. Jin, "Aoas and aods estimation for sparse millimeter wave channels with one-bit adcs," in *2016 8th International Conference on Wireless Communications Signal Processing (WCSP)*, 2016, pp. 1–5.

[183] C. Stckle, J. Munir, A. Mezghani, and J. A. Nossek, "1-bit direction of arrival estimation based on compressed sensing," in *2015 IEEE 16th International Workshop on Signal Processing Advances in Wireless Communications (SPAWC)*, 2015, pp. 246–250.

[184] C. Rusu, N. Gonzlez-Prelcic, and R. W. Heath, "Low resolution adaptive compressed sensing for mmwave mimo receivers," in *2015 49th Asilomar Conference on Signals, Systems and Computers*, 2015, pp. 1138–1143.

[185] C. Rusu, R. Mendez-Rial, N. Gonzalez-Prelcic, and R. W. Heath, "Adaptive one-bit compressive sensing with application to low-precision receivers at mmwave," in *2015 IEEE Global Communications Conference (GLOBECOM)*, 2015, pp. 1–6.

[186] A. M. Sayeed, "Deconstructing multiantenna fading channels," *IEEE Transactions on Signal Processing*, vol. 50, no. 10, pp. 2563–2579, 2002.

[187] T. M. Lok and V. K. . Wei, "Channel estimation with quantized observations," in *Proceedings. 1998 IEEE International Symposium on Information Theory (Cat. No.98CH36252)*, 1998, pp. 333–.

[188] L. Jacques, J. N. Laska, P. T. Boufounos, and R. G. Baraniuk, "Robust 1-bit compressive sensing via binary stable embeddings of sparse vectors," *IEEE Transactions on Information Theory*, vol. 59, no. 4, pp. 2082–2102, 2013.

[189] U. S. Kamilov, A. Bourquard, A. Amini, and M. Unser, "One-bit measurements with adaptive thresholds," *IEEE Signal Processing Letters*, vol. 19, no. 10, pp. 607–610, 2012.

[190] S. Rangan, "Generalized approximate message passing for estimation with random linear mixing," in *2011 IEEE International Symposium on Information Theory Proceedings*, 2011, pp. 2168–2172.

[191] J. P. Vila and P. Schniter, "Expectation-maximization gaussian-mixture approximate message passing," *IEEE Transactions on Signal Processing*, vol. 61, no. 19, pp. 4658–4672, 2013.


This work is licensed under a Creative Commons Attribution 4.0 License. For more information, see https://creativecommons.org/licenses/by/4.0/.

This article has been accepted for publication in a future issue of this journal, but has not been fully edited. Content may change prior to final publication. Citation information: DOI 10.1109/OJCOMS.2020.3015394, IEEE Open Journal of the Communications Society



[192] C. Guo and M. E. Davies, "Near optimal compressed sensing without priors: Parametric sure approximate message passing," *IEEE Transactions on Signal Processing*, vol. 63, no. 8, pp. 2130–2141, 2015.

[193] S. Rangan, P. Schniter, and A. K. Fletcher, "Vector approximate message passing," *IEEE Transactions on Information Theory*, vol. 65, no. 10, pp. 6664–6684, 2019.

[194] P. Schniter, S. Rangan, and A. K. Fletcher, "Vector approximate message passing for the generalized linear model," in *2016 50th Asilomar Conference on Signals, Systems and Computers*, 2016, pp. 1525–1529.

[195] C. Stckle, J. Munir, A. Mezghani, and J. A. Nossek, "Channel estimation in massive mimo systems using 1-bit quantization," in *2016 IEEE 17th International Workshop on Signal Processing Advances in Wireless Communications (SPAWC)*, 2016, pp. 1–6.

[196] J. T. Parker, P. Schniter, and V. Cevher, "Bilinear generalized approximate message passingpart i: Derivation," *IEEE Transactions on Signal Processing*, vol. 62, no. 22, pp. 5839–5853, 2014.

[197] S. Rao, A. L. Swindlehurst, and H. Pirzadeh, "Massive mimo channel estimation with 1-bit spatial sigma-delta adcs," in *ICASSP 2019 - 2019 IEEE International Conference on Acoustics, Speech and Signal Processing (ICASSP)*, 2019, pp. 4484–4488.

[198] Y. Li, C. Tao, G. Seco-Granados, A. Mezghani, A. L. Swindlehurst, and L. Liu, "Channel estimation and performance analysis of one-bit massive mimo systems," *IEEE Transactions on Signal Processing*, vol. 65, no. 15, pp. 4075–4089, 2017.

[199] S. Jacobsson, G. Durisi, M. Coldrey, U. Gustavsson, and C. Studer, "One-bit massive mimo: Channel estimation and high-order modulations," in *2015 IEEE International Conference on Communication Workshop (ICCW)*, 2015, pp. 1304–1309.

[200] K. Roth, H. Pirzadeh, A. L. Swindlehurst, and J. A. Nossek, "A comparison of hybrid beamforming and digital beamforming with low-resolution adcs for multiple users and imperfect csi," *IEEE Journal of Selected Topics in Signal Processing*, vol. 12, no. 3, pp. 484–498, 2018.

[201] A. Kabiri, M. J. Emadi, and M. N. Khormuji, "Optimal design of semi-orthogonal multiple-access massive mimo systems," *IEEE Communications Letters*, vol. 21, no. 10, pp. 2230–2233, 2017.

[202] L. Dai, B. Wang, Z. Ding, Z. Wang, S. Chen, and L. Hanzo, "A survey of non-orthogonal multiple access for 5g," *IEEE Communications Surveys Tutorials*, vol. 20, no. 3, pp. 2294–2323, 2018.

[203] P. Ioannides and C. A. Balanis, "Uniform circular and rectangular arrays for adaptive beamforming applications," *IEEE Antennas and Wireless Propagation Letters*, vol. 4, pp. 351–354, 2005.

[204] S. Ghosh and D. Sen, "An inclusive survey on array antenna design for millimeter-wave communications," *IEEE Access*, vol. 7, pp. 83 137–83 161, 2019.

[205] D. Zhang, A. Li, M. Shirvanimoghaddam, P. Cheng, Y. Li, and B. Vucetic, "Codebook-based training beam sequence design for millimeter-wave tracking systems," *IEEE Transactions on Wireless Communications*, vol. 18, no. 11, pp. 5333–5349, 2019.

[206] S. Shaham, M. Ding, M. Kokshoorn, Z. Lin, S. Dang, and R. Abbas, "Fast channel estimation and beam tracking for millimeter wave vehicular communications," *IEEE Access*, vol. 7, pp. 141 104–141 118, 2019.

[207] Y. Song, W. Yang, X. Yang, Z. Xiang, and B. Wang, "Physical layer security in cognitive millimeter wave networks," *IEEE Access*, vol. 7, pp. 109 162–109 180, 2019.

[208] C. G. Tsinos, S. Chatzinotas, and B. Ottersten, "Hybrid analog-digital transceiver designs for multi-user mimo mmwave cognitive radio systems," *IEEE Transactions on Cognitive Communications and Networking*, vol. 6, no. 1, pp. 310–324, 2020.

[209] Y. Song, W. Yang, Z. Xiang, N. Sha, H. Wang, and Y. Yang, "An analysis on secure millimeter wave noma communications in cognitive radio networks," *IEEE Access*, vol. 8, pp. 78 965–78 978, 2020.

This work is licensed under a Creative Commons Attribution 4.0 License. For more information, see https://creativecommons.org/licenses/by/4.0/.